ALMA MATER STUDIORUM - UNIVERSITÀ DI BOLOGNA

SCUOLA DI INGEGNERIA E ARCHITETTURA

Dipartimento di ingegneria civile, chimica, ambientale e dei materiali (DICAM)

CORSO DI LAUREA MAGISTRALE IN IGNEGNERIA CHIMICA E DI PROCESSO

TESI DI LAUREA

in

Thermodynamics of Energy and Materials

Modeling of a differential volumetric system for high pressure gas adsorption

CANDIDATE:
Giacomo De Angelis

SUPERVISOR:
Prof. Marco Giacinti Baschetti

CO-SUPERVISOR:
Prof. Enzo Mangano
Ing. Riccardo Rea

Anno Accademico 2019/2020

Sessione III

Abstract

The volumetric system is a widely used experimental method for gas adsorption equilibrium measurements and for the determination of adsorption kinetics. A predictive model was developed in the gPROMS ProcessBuilder platform.

Equations for mass and energy balance were implemented firstly for the description of a single-branch volumetric apparatus, and then for a differential (double-branched) system.

The model was built starting from the simplest case (Isothermal and ideal gas behaviour) and subsequentially its complexity was increased in order to have a system which is able of describing an adsorption process in any operative conditions (non-isothermal system, non-linear equilibrium, real gas behaviour).

The validation of the model was made through the assumption that all the complex systems must collapsed to the simplest one through the adjustment of the different parameters. In certain cases, the validation was done comparing the results obtained in the simulation with the one got from analytical solutions developed by other authors.

In general, at the end of each section, a case study was analysed in order to underline what are the factors that can affect the kinetic of the process, providing also possible solution which can minimize these effects, that if not taken into account can lead to an incorrect interpretation of the data.

Keywords: Adsorption - gPROMS - Modeling - Volumetric method - Differential pressure adsorption

Table of Contents

1. Introduction

The growing demand for energy and environmental problem due to the pollutant energy sources imposes on E.U. and U.S. governments, and science the need to look for new and clean energy-carrier resources. In this aspect hydrogen and methane gas are considered one of the most promising candidates to achieve this goal. While their production and delivery have reached a sufficient development level, there is a lot of room of improvement on storage and portability (Policicchio, et al., 2013). In this sense, one of the main techniques that could be used, not only for the storage, but also in the development of new materials addressing to the storage, is the adsorption process, in particular high-pressure adsorption technique.

1.1 Motivation

The aim of this thesis project is the building of a mathematical model that is able to describe an adsorption process in a volumetric system in any operative conditions, through the implementation of *partial differential equations (PDEs)* and *ordinary differential equations (ODEs)***.**

The model can be used as a predictive tool by the operator to decide what are the best conditions to carried out an experiment, in order to study the adsorption characteristics of a certain material.

1.2 Thesis Outline

Firstly, in Chapter 2, a literature review was made where is present a description of the different type of adsorption methods that can be used. In particular, a focus is made to the volumetric and differential volumetric techniques. Then, is present a description of the software platform

in which all the modeling was made on. At last, a short definition of the equations of state and how they can be classified.

In Chapter 3, a mathematical model for a volumetric single-branch apparatus was implemented, starting from the simplest case and then the different complexity were added. In general, before the description of any single case a flowchart is used to define all the assumptions considered, represented through green boxes. and then a validation of the results was made, followed by some interesting cases study. Moving on Chapter 4 is described the mathematical model for a volumetric double-branch apparatus. For this new model, some case studies already seen for the single-branch apparatus are analysed.

Finally, Chapter 5 summarizes the main conclusions with the present work and discusses all the future work that needs to be addressed.

2. Background

2.1 Volumetric system

Adsorption is the adhesion of atoms, ions or molecules from a gas, liquid or dissolved solid to a surface. The liquid or gas is called as the *adsorbate* and the surface on which it adsorbs is called as *adsorbent.* The adsorption is a surface phenomenon where the adsorbate molecules adhere to the micropores on the surface of the adsorbent material. The primary requirement for a convenient process is an adsorbent with sufficiently high *selectivity.* In general, for an adsorption process, it is possible to distinguish between physical adsorption, involving only relatively weak intermolecular forces, and chemisorption which involves the formation of a chemical bond between the sorbate molecule and the surface of the adsorbent. The heat of adsorption provides a direct measure of the strength of the bonding between sorbate and surface. And, through the use of the thermodynamic, it is possible to demonstrate that physical

adsorption from the gas phase is always exothermic. Since the adsorbed molecule has at most two degrees of translational freedom on the surface and since the rotational freedom of the adsorbed species must always be less than that of the gas phase molecules, the entropy change on adsorption ($\Delta S = S_{ads} - S_{gas}$) is negative. Furthermore, since the free energy change on adsorption (ΔG) must be negative and since $\Delta G = \Delta H - T\Delta S$ this requires a negative enthalpy (Ruthven, 1984).

***Table 1**: Features of physical adsorption and chemisorption (Ruthven, 1984)*

PHYSICAL ADSORPTION	CHEMISORPTION
Low heat of adsorption (< 2 or 3 times latent heat of evaporation)	High heat of adsorption (> 2 or 3 times latent heat of evaporation)
Non Specific	Highly Specific
Monolayer or multilayer	Monolayer only
No dissociation of adsorbed species	May involve dissociation
Only significant at relatively low temperatures	Possible over a wide range of temperature
Rapid, non-activated, reversible	Activated, may be slow and irreversible
No electron transfer although polarization of sorbate may occur	Electron transfer leading to bond formation between sorbate and surface

The amount adsorbed can be measured in at least two ways: by measuring the change in weight of the solid with a spring balance or measuring the change in pressure of the gas in an accurately known volume, knowing the sample of the volume; these techniques are called *gravimetric* and *volumetric***,** respectively.

The second method represents the most common technique for determining the adsorption uptake of gas by a solid material. As shown in Fig. 1, the simplest instrument consists of two accurately known volumes, the dosing and the uptake cells, separated by a valve -which is one

of the most important elements of the system- exposed to a pressure measurement device, and held at a constant temperature T. Despite the high importance that the valve has in the kinetics of the process, an aspect that will be explored more specifically later, very few systems include its dynamics (Wang, Mangano, Brandani, & Ruthven, 2020).

The attractive feature of a volumetric experiment is its robustness and relatively low cost, especially comparing a good pressure transducer to an electronic microbalance, uses in the gravimetric experiments. The sample, whose volume is also known, is placed in the uptake cell.

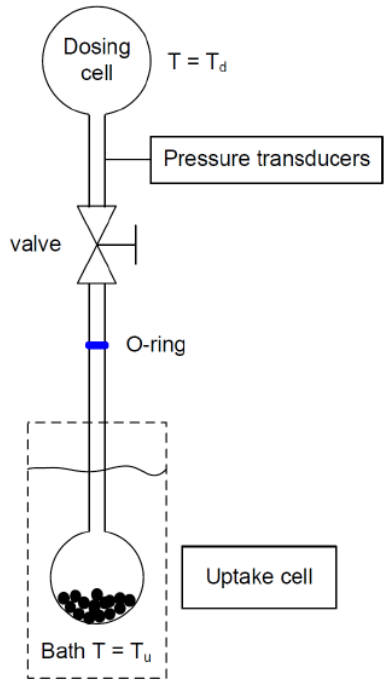

***Figure 1**: Schematic representation of a volumetric system (Brandani, 2019)*

To increase sensitivity the volumes of the two sides could be optimised with V_u kept to a minimum, but in practice one needs some distance between the valve and the sample to allow high temperature regeneration and pre-conditioning of the sample, this means that, usually, the ratio of V_d/V_u is typically between 0.5 and 1. Between the valve and the sample a filter is normally placed, and it is used to avoid contamination of the dosing volume, which requires a significance downtime and careful maintenance. The filter could be represents the main resistance to the gas flow.

Measurement of a single value of the equilibrium adsorption uptake at a certain pressure and temperature requires two steps (Stadie, 2013). In the first one, a certain quantity of gas is put in the dosing cell (n_m). This initial amount is the total amount of gas that will be available for adsorption in the second step and can be determined from the Ideal gas law. After equilibration, the valve is opened and the gas is expanded into the uptake cell, where it is exposed to the sample. Some quantity of gas (n_{ads}) will be adsorbed by the sample and removed from the gas phase. Pressure is monitored until it stabilizes, indicating adsorption has equilibrated, then the equilibration pressure (P_e) is recorded. The quantity of gas (n_e) remaining in the dosing and uptake cells ($V_d + V_u$) can be calculated, also in this case, from the Ideal gas law. Once n_e is determined, the quantity of gas adsorbed by the sample at P_e is:

$$n_{ads} = n_m - n_e \tag{2.1}$$

This establishes the point on the isotherm (P_e,n_{ads}). Then the valve is closed, and the dosing cell is charged to a pressure slightly higher than P_e after which the entire process is repeated. This cycle continues until the analysis pressure is near saturation pressure at which time the complete adsorption isotherm has been developed (MIC, 2005).

Mostly of the commercial systems are also used to measure BET surface at 77 K, and in general apparatuses differ on the basis of how the liquid level is controlled. For example, in many systems the sample side is submerged in a thermal fluid and the liquid level is tracked as the fluid evaporates (Wang, Mangano, Brandani, & Ruthven, 2020).

Despite exist a large number of publications which provide reliable data for low-pressure adsorption experiments, the same cannot be said for high-pressure analysis. In general, high-pressure adsorption measurements are more difficult to be achieved than low pressure-ones, leading to a lack of standardized protocols, reference materials and reference data (Nguyen, et al., 2018).

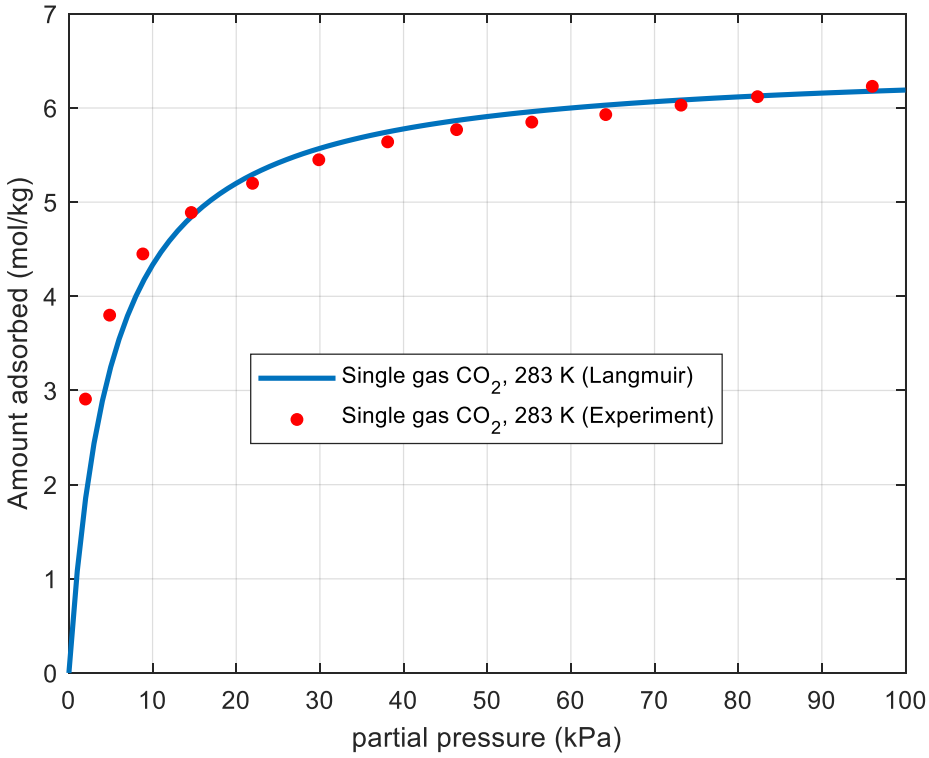

***Figure 2**: Example of isotherm related to the adsorption of carbon dioxide on 13X zeolite (Shigaki, Mogi, Haraoka, & Furuya)*

For volumetric systems it is essential to ensure that leak rates are kept to a minimum and, as much as possible, reduced to zero. Metal gaskets and stainless-steel fittings can be used for this purpose, but in the low-pressure commercial systems the sample is inserted in a glass cell that is sealed with a polymeric o-ring (represented in blue in the Fig. 1). However, leak tests should be made in order to ensure that the system has a stable pressure. Indeed, if the leak rate is not negligible or if the equilibration time is too short an apparent open hysteresis should be observed. Also for high-pressure measurements is important to minimize any leaks because they can lead to the enter of water inside the system affecting measurements for hydrophilic materials (Wang, Mangano, Brandani, & Ruthven, 2020).

2.2 Differential Volumetric system

One of the main problems in the use of a volumetric apparatus for the adsorption experiments is the loss of accuracy when high pressure adsorption measurements are carried out, in particular considering weakly-adsorbing light gases such as hydrogen. In general, these types of experiments have been conducted on high pressure volumetric adsorption unit known as a *Sieverts apparatus* (Sircar, Wang, & Lueking, 2013) **.** Indeed, at high pressures, the apparatus is very sensitive to temperature instability, leaks and additional pressure and temperature effects caused by expanding the gas from the reservoir to the sample cell. This combined with a possible inconsistency of the materials studied has led to a wide range of results (Blackman, Patrick, & Colin, 2005).

A second volumetric approach has been introduced using the measurement of differential pressure in an attempt to improve the accuracy and reliability of the method. A differential unit consists of two mirror-image single-sided units connected via a differential pressure transducer, so that adsorption and blank experiments may be conducted simultaneously. The differential apparatus determines the amount of gas adsorbed by a material based on a differential pressure change between a reference cell and a sorption cell containing the sample.

Sorption experiments are initiated by charging the sample and reference side manifolds with gas, allowing time to come to thermal equilibrium, and subsequently expanding to the sample and reference cells, and the resulting difference in pressure between the two cells is monitored. After equilibration, the manifolds are repressurized and expanded again.

Sorption capacities are determined via mass balance, taking into account the non-ideality of the gas phase through the use of an equation of state (Zielinski, et al., 2007).

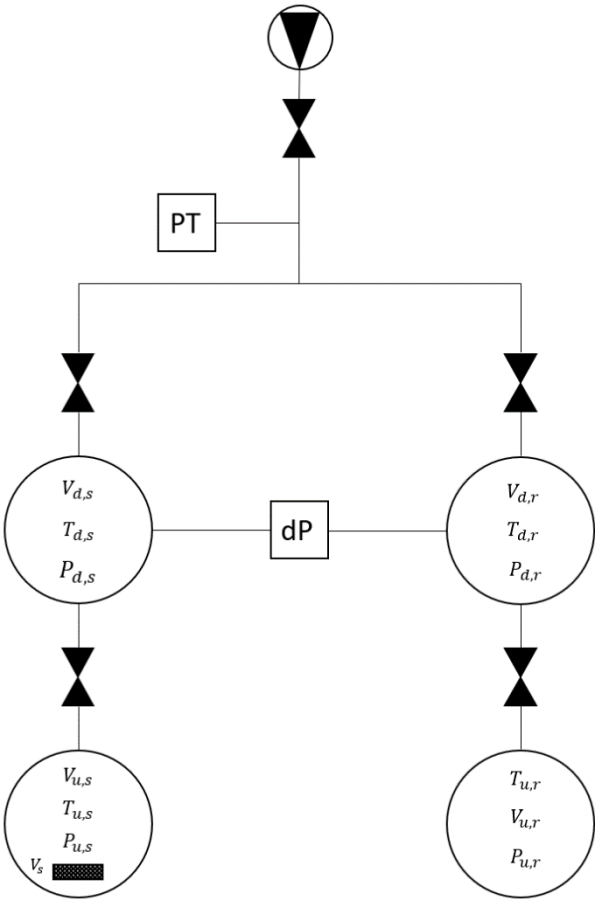

***Figure 3**: Schematic representation of a differential volumetric apparatus*

This technique is claimed to have several advantages over the traditional direct pressure measurement. Firstly, differential pressure transducers (dP in Fig. 3) are far more precise (measure to ca. 0.001 bar) than absolute high-pressure transducers (measure to ca. 0.01 bar) operating at high pressure and consequently the accuracy of the pressure monitoring system is higher. The method also attempts to eradicate many of the problems associated with the expansion of non-ideal gas, which can introduce large errors when performing this type of measurements, by using simultaneous expansions in the sample and reference cells (Blackman, Patrick, & Colin, 2005).

2.3 gPROMS: An Equation Oriented Tool for Modeling Simulation and Optimisation

gPROMS is a **g**eneral **PRO**cess **M**odeling **S**ystem model builder with capabilities for the simulation for dynamics and steady state, optimization, experiment design and parameter estimation of any type of process (Gosling, 2005).

gPROMS uses high-level language to describe a complex process based on the equation-oriented technology, moreover, it has built-in a numerical solver for process simulation and optimization problems. The program is used for a wide range of applications in petrochemical, food, pharmaceutical, and in particular in chemicals and automation. But in general, it can be used for any type of process that can be illustrated by a set of mathematical equations, including (PSe, 2004):

- Dynamic simulation
- Steady-state simulation
- Dynamic optimisation
- Steady-state optimisation
- Dynamic parameter estimation
- Steady-state parameter estimation

gPROMS has many advantages that make it an attractive tool for solving dynamic and steady-state modeling problems, such as: clear and concise language, unparalleled modeling power and the ability to model process discontinuities and operating conditions among many other. One of the most important advantage of the program is the possibility to write equations almost as they would appear on paper. The clear, concise language allows the user to concentrate on getting the modeling equations correct while not having to be concerned with the complexity of the solution techniques. Other important features of gPROMS are (PSe, 2004):

- The capability to handle a huge number of algebraic and differential equations, and over 100,000 equations can be simulated
- gPROMS can be used for the same model for different simulation and optimization activity
- It can be readily integrated with most of the automation software such as HYSYS, MatLab and Simulink
- It is a clear and concise language, unparalleled modeling power and with the ability to model process discontinuities and operating conditions among many others

The gPROMS model builder has different number of entries, where the most important are:

- Variable types
- Stream types
- Tasks
- Processes
- Optimisation
- Parameter estimation
- Experimental design

For this work just three of these sections are used, and they are: *Variable types* entry which is used to specify the types and range of the variables; *Model*, where different sections can be identified. Such as the one related to the parameter, where the constant values are reported. The section of the variable is used to declare the variables of the model, and the equation section is used to declare the equations that determine the time trajectories of the variables. Then, the *Processes* section contains specification for the simulation of the specific process.

Model is defined as the modeling of chemical, physical and biological plant behaviour. Generally, any gPROMS Model is described in the following:

- Three types of constant (REAL, INTEGER, LOGICAL) that clarify the system. They are declared in the *Parameter* section. These values should be provided before simulation start
- Variables and corresponding variable type of the model that may or may not vary with time are declared in the *Variable* section
- A set of equations involving both the differential and algebraic, are declared in the *Equation* section

2.4 Equations of State (EoS)

In general, it is possible to say that an Equation of State is the relation between functions of state, such as temperature (T), pressure (P), volume (V), internal energy or specific heat. It characterizes the state of matter of a material under a given set of physical conditions.

In the limit of low pressures and high temperatures, where the molecules of gas move independently of one another, the behaviour of the gas can be easily predicted using the well-known ideal gas law: $PV = nRT$.

However, at high pressure and at low temperature, real gases deviate from the ideality and the equation need to be modified. In order to write an equation of state for a real gas, a correction factor has to be inserted into the ideal gas equation, known as compressibility factor (Z) (Mansour, 2020). It says how much the thermodynamic properties of a real gas deviate from the one of the ideal counterpart. All Eos are based on assumptions, and they are tested by their ability to reproduce the experimental data. There are different types of EoS which can be grouped into three different groups:

- **First class of EoS**: these equations are cubic equation of state. The cubic equations of state, such as the Van der Waals, Redlich and Kwong, RKS and Peng-Robinson equations, give reasonable results for the thermodynamic behaviour of real fluids. In

particular for the calculation of vapor pressures and equilibrium phase composition mixtures, the use of cubic equations is quite functional as they yield fairly accurate results (Kunz, Klimeck, Wagner, & Jaeschke, 2007)

- **Second class of EoS**: these EoS are non-cubic in form. They provide accurate results for both vapor and liquid phases
- **Third class of EoS**: these are non-analytical Eos that are highly constrained for some specific fluid and are capable of expressing real fluid thermodynamic properties precisely

Usually, the first class EoS is more useful because it provides an analytical solution than the more complex non-cubic second type and non-analytical type.

In this work will be used two different equations of state to describe the real behaviour of gases: Peng-Robinson and van der Waals equation of state.

Indeed, even if exist models much more complicated than these (Span & Wagner, 1996), the most important advantage of the cubic equation of state is their simple mathematical structure and reliability, in particular for the evaluation of corresponding experimental data (Kunz, Klimeck, Wagner, & Jaeschke, 2007).

3. Modeling of a Volumetric system in a single-branch apparatus

Mathematical modeling in engineering is concerned with the use of mathematical equations to predict the actual process behaviour. There are different advantages of using the model and simulation rather than using experimental work or real operations, some of these are, for example:

- Use of a model saves time
- It is cheaper than using a real process
- Computer simulation and optimization saves money in design and operation

Can be identified two type of process models: a steady-state and a dynamic model. In the first case no change in process variables with time is considered, while the dynamic model depends on time; in this work, a dynamic model for the adsorption process is developed. The model includes some parameters such as the volume of the dosing and uptake cells, intracrystalline diffusivity, mass of solid and radius of sample.

3.1 Isothermal case of a single-branch Volumetric system

3.1.1 Process Description & Mathematical Model

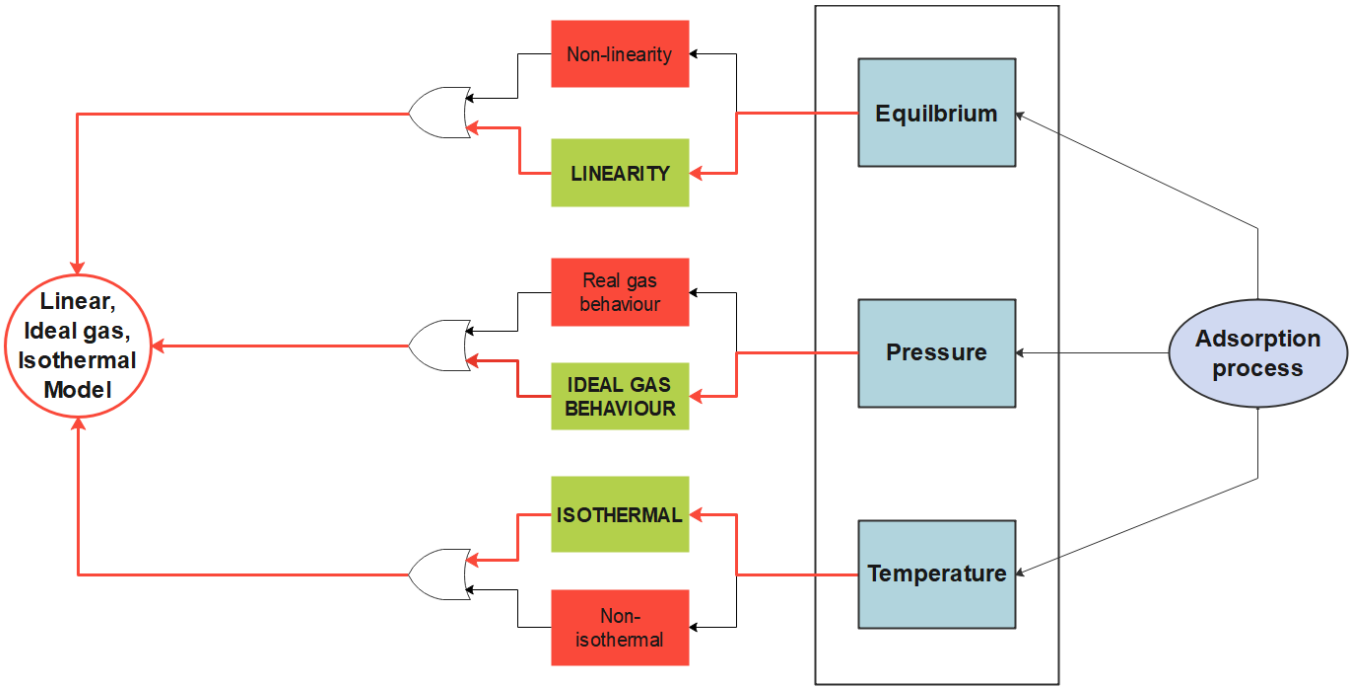

***Figure 4**: Pathway map of the model*

All volumetric systems are based on the expansion of a gas between a dosing volume and an uptake cell, which contains the sample, Fig. 5 represents a schematic configuration of a volumetric system. As was already explained, the experiment consists in closing the valve and changing the pressure in the dosing cell for either an adsorption or a desorption experiment. The valve is then opened and the pressure in the dosing cell monitored in time (Wang, Mangano, Brandani, & Ruthven, 2020).

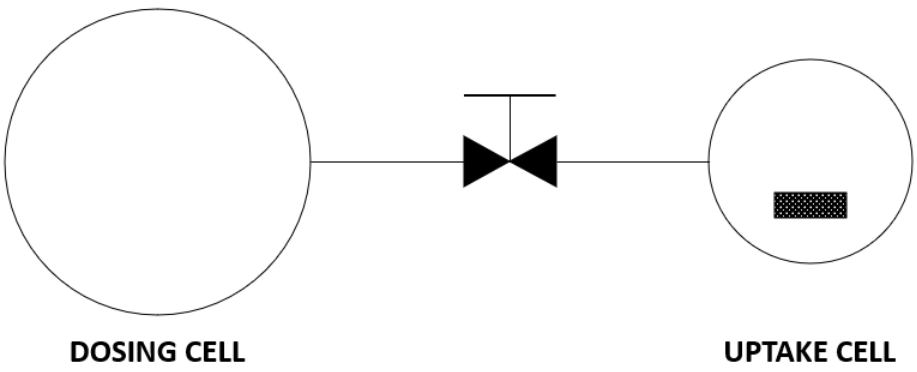

***Figure 5**: schematic representation of a volumetric system (Brandani, 1998)*

One of the basic problems that must be considered is the flow of the gas through the valve, for this reason were considered only small pressure differences, in order to obtain a linearized expression for the flow through the valve. And this is valid in particular considering very strongly adsorbed species (Brandani, 1998). In this sense, the following equation for the flow through the valve was used:

$$\frac{dn}{dt} = \chi_t \chi (P_d^2 - P_u^2) \tag{3.1}$$

Where P_d and P_u are the pressures in the dosing and uptake cells, χ is the valve constant and χ_t is a time dependent function which describes the opening of the valve. In order to establish the limits of applicability of the technique, it is possible to simplify the problem considering the valve ideal, so with a zero-opening time. Indeed, the opening of the valve imposes a further limitation on the mass flow to the uptake volume. Considering also a small pressure difference the previous equation can be rewritten as:

$$\frac{dn}{dt} \cong \chi (P_d^0 + P_u^0)(P_d - P_u) = \bar{\chi}(P_d - P_u) \tag{3.2}$$

The following mass balance was applied to the uptake volume (V_u):

$$V_s \frac{d\bar{q}}{dt} + \varepsilon V_u \frac{dc}{dt} = \frac{dn}{dt} \tag{3.3}$$

Where V_s is the volume of the sample, $\bar{q}$ is the average adsorbed phase concentration, c is the gas phase concentration and ε is the void fraction in the uptake cell.

While, for the dosing volume (V_d) the mass balance applied is:

$$\frac{dn}{dt} = -\frac{V_d}{R_g T_d} \frac{dP_d}{dt} \tag{3.4}$$

Where R_g is the ideal gas constant and T_d is the temperature of the dosing cell. In low pressure experiments it is possible to assume an ideal gas behaviour and $c = \frac{P_u}{\mathcal{R} T_u}$.

The solid phase mass balance, considering spherical particles, is given by:

$$\frac{\partial q}{\partial t} = D\left(\frac{\partial^2 q}{\partial r^2} + \frac{2}{r}\frac{\partial q}{\partial r}\right) \tag{3.5}$$

and

$$\frac{d\bar{q}}{dt} = \frac{3D}{R}\left(\frac{\partial q}{\partial r}\right)_{r=R} \tag{3.6}$$

Where D is the diffusivity coefficient and R is the radius of the crystals.

As boundary conditions for the solid phase mass balance, were considered equilibrium at the surface between the adsorbed phase and the gas phase, and the symmetry condition:

$$\left(\frac{\partial q}{\partial r}\right)_{r=0} = 0 \tag{3.7}$$

Was assumed also a linear equilibrium relationship:

$$q(R,t) - q_0 = K(c(t) - c_0) \tag{3.8}$$

Where K is the equilibrium constant.

The Henry model assumes that adsorption is directly proportional to solute concentration in a solution. However, one of the most limiting factors of this model is its strict application to low solute concentrations. Other factors assumed by this model are (Martinez-Vertel, et al., 2018):

- Energy levels on the surface are equivalent so there is not any preference of the adsorbate to occupy a specific place on the adsorbent
- The surface is infinite. The reason for this assumption is based on the fact that the solute concentration is so low that if it is compared to the available adsorbent surface, the adsorbate can be retained with no restriction
- There is no interaction between molecules once they are adsorbed
- The type of adsorption occurring is a monolayer adsorption due to the low concentration of solute utilized

Introducing the following dimensionless variables and dimensionless parameters:

***Table 2**: dimensionless variables and parameters*

Dimensionless variables
$\tau = \frac{tD}{R^2}$ $\quad Q = \frac{q - q_0}{q_\infty - q_0}$ $\quad C = \frac{c - c_0}{c_\infty - c_0}$
$\rho_d = \frac{P_d - P_u^0}{P_\infty - P_u^0}$ $\quad \rho_u = \frac{P_u - P_u^0}{P_\infty - P_u^0}$
Dimensionless parameters
$\gamma = \frac{\epsilon V_u}{3HV_s}$ $\quad \delta = \frac{V_d}{3HV_s}$ $\quad \omega = \frac{\mathcal{R}T_d\bar{\chi}R^2}{V_d D}$

It is possible to rewrite the governing equations in dimensionless form:

$$\frac{d\rho_d}{d\tau} = \omega(\rho_u - \rho_d) \tag{3.9}$$

$$\gamma\frac{d\rho_u}{d\tau} + \delta\frac{d\rho_d}{d\tau} + \left(\frac{\partial Q}{\partial \xi}\right)_{\xi=1} \tag{3.10}$$

With $\xi = \frac{r}{R}$ and

$$\frac{\partial Q}{\partial \tau} = \frac{\partial^2 Q}{\partial \xi^2} + \frac{2}{\xi}\frac{\partial Q}{\partial \xi} \tag{3.11}$$

With initial and boundary conditions given by

$$Initial\ conditions \begin{cases} \rho_d(0) = \rho_d^0 \\ \rho_u(0) = 0 \\ Q(\xi, 0) = 0 \end{cases}$$

$$Boundary\ conditions \begin{cases} Q(0,\tau) = 0 \\ Q(1,\tau) = \rho_u(\tau) \end{cases}$$

As was already stated, for this system the effect of the valve between the two volumes must be considered in order to study the real dynamic of it. In this sense, instead converting the data to a fractional uptake, it is much better to plot a normalized pressure, express as reduced pressure (Brandani, Brandani, Mangano, & Pullumbi, 2019):

$$\sigma_D = \frac{P_D - P_\infty}{P_D^0 - P_\infty} = \frac{\rho_D (P_\infty - P_U^0) + P_U^0 - P_\infty}{P_D^0 - P_\infty} \tag{3.12}$$

Defined in this way the dimensionless pressure in the dosing cell varies between 1 and 0. If this is plotted versus time on a semilog plot, it is possible to identify the short-time initial decay which is dependent from the dynamic of the valve, and the long-time asymptote which depends only from the diffusion time constant $\frac{R^2}{D}$. It is important to clarify that the effect of the valve takes into account also the time required to the gas to diffuse in the tube between the dosing cell and the sample; so, the tube length affects the value of the constant, even if the valve is considered instantaneous.

Furthermore, the semilog plot of the reduced pressure of the dosing cell provides also a direct way to determine if the process is a diffusion process or is controlled by a surface barrier (Brandani, Brandani, Mangano, & Pullumbi, 2019).

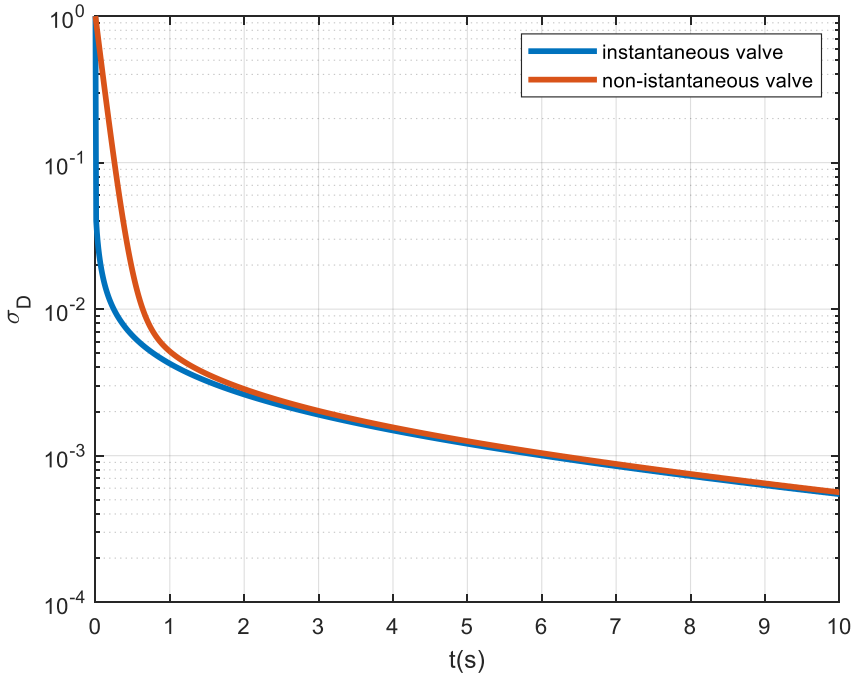

***Figure 6**: effect of the valve on the trend of the reduced pressure*

3.1.2 Model Validation

The case study reported by Brandani (1998) is used here for model validation, in particular comparing the results obtained from the simulation with the analytical solution of a piezometric system under isothermal condition developed by the author; the solution to the governing equations is given by:

$$\frac{\rho_d}{\rho_d^0} = \frac{3\delta}{1+3\delta+3\gamma} + \sum_{i=0}^{\infty} a_i \exp\left(-\beta_i^2 \tau\right) \tag{3.13}$$

And

$$\frac{\rho_u}{\rho_d^0} = \frac{3\delta}{1+3\delta+3\gamma} + \sum_{i=0}^{\infty} a_i \left(1 - \frac{\beta_i^2}{\omega}\right) \exp\left(-\beta_i^2 \tau\right) \tag{3.14}$$

Where

$$a_i = \frac{2\omega^2 \delta \beta_i^2}{2\omega^2 \delta \beta_i^2 + (\omega - \beta_i^2)^2 (\beta_i^2 + z_i^2 - z_i + 2\gamma\beta_i^2)} \tag{3.15}$$

and β_i are the positive nonzero roots of

$$\beta_i \cot \beta_i - z_i = 0 \tag{3.16}$$

The curves calculated from the equation related to the dimensionless pressure in the dosing volume, all decrease monotonically to the final equilibrium value. On the other hand, the curves calculated from the equation of the dimensionless pressure in the uptake cell may be exhibit a maximum, allowing a clear qualitative indication of a kinetically controlled process when the pressure in the uptake cell is monitored. As a first representative example was considered the case where $\gamma = \delta = 0.01$ (which is a typical value for a substance that is not strongly adsorbed) for a range of different values of the parameter ω (which is basically the ratio of the time constants for the valve opening and for intracrystalline diffusion). For the analysis were considered also the limiting curves for equilibrium control and for empty cell, whose equations are:

$$\frac{\rho_d}{\rho_d^0} = \frac{3\delta}{1+3\delta+3\gamma} + \frac{1+3\gamma}{1+3\delta+3\gamma}\exp\left(-\frac{1+3\delta+3\gamma}{1+3\gamma}\omega\tau\right) \tag{3.17}$$

$$\frac{\rho_u}{\rho_d^0} = \frac{3\delta}{1+3\delta+3\gamma} \times \left(1 - \exp\left(-\frac{1+3\delta+3\gamma}{1+3\gamma}\omega\tau\right)\right) \tag{3.18}$$

And in the absence of adsorbent

$$\frac{\rho_d}{\rho_d^0} = \frac{\delta}{\delta+\gamma} + \frac{\gamma}{\delta+\gamma}\exp\left(-\frac{\delta+\gamma}{\gamma}\omega\tau\right) \tag{3.19}$$

$$\frac{\rho_u}{\rho_d^0} = \frac{\delta}{\delta+\gamma} \times \left(1 - \exp\left(-\frac{\delta+\gamma}{\gamma}\omega\tau\right)\right) \tag{3.20}$$

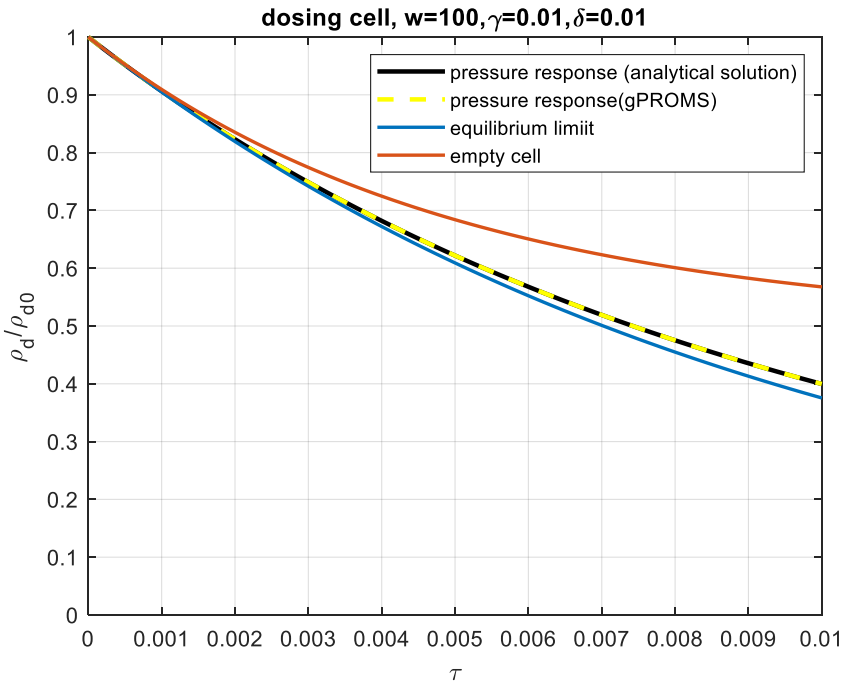

***Figure 7**: pressure response in dosing cell with ω=100*

Analysing the curve above, it is possible to observe that there are only small differences between the kinetically controlled response and the limiting curves for equilibrium control. Furthermore, the difference from the equilibrium controlled curve is greater in the final stage of the approach to equilibrium.

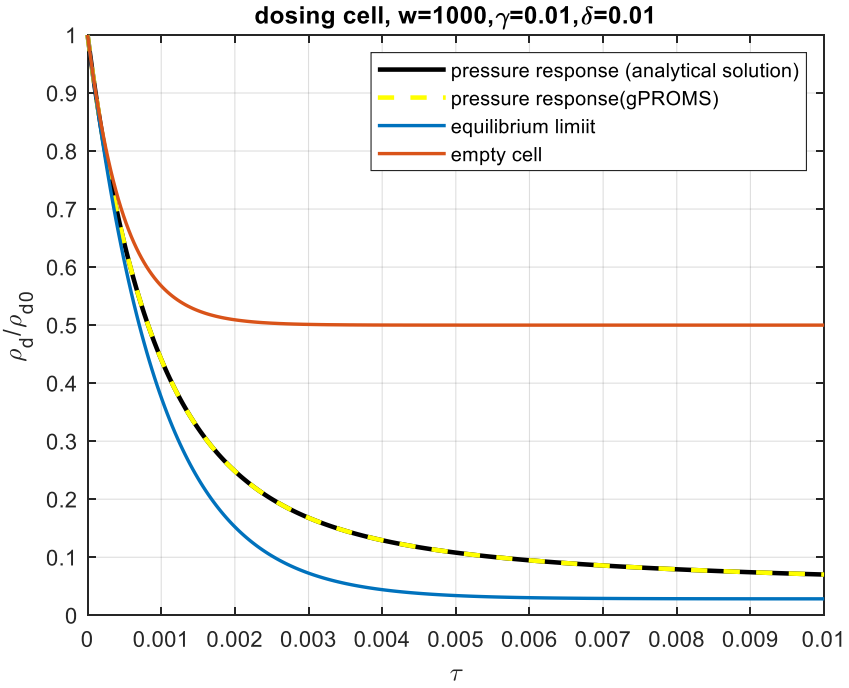

***Figure 8**: pressure response in dosing cell with ω =1000*

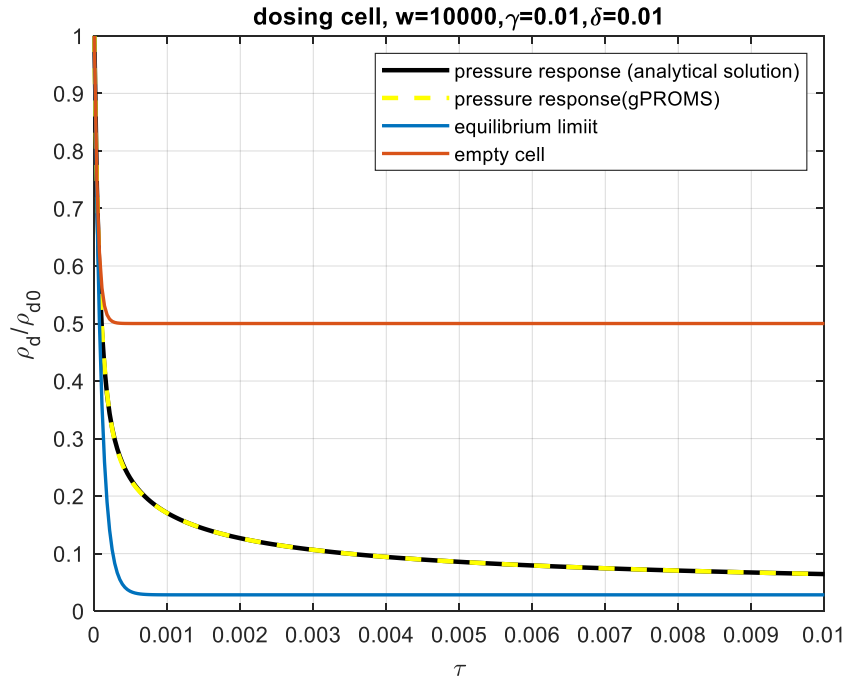

***Figure 9**: pressure response in dosing cell with ω =10000*

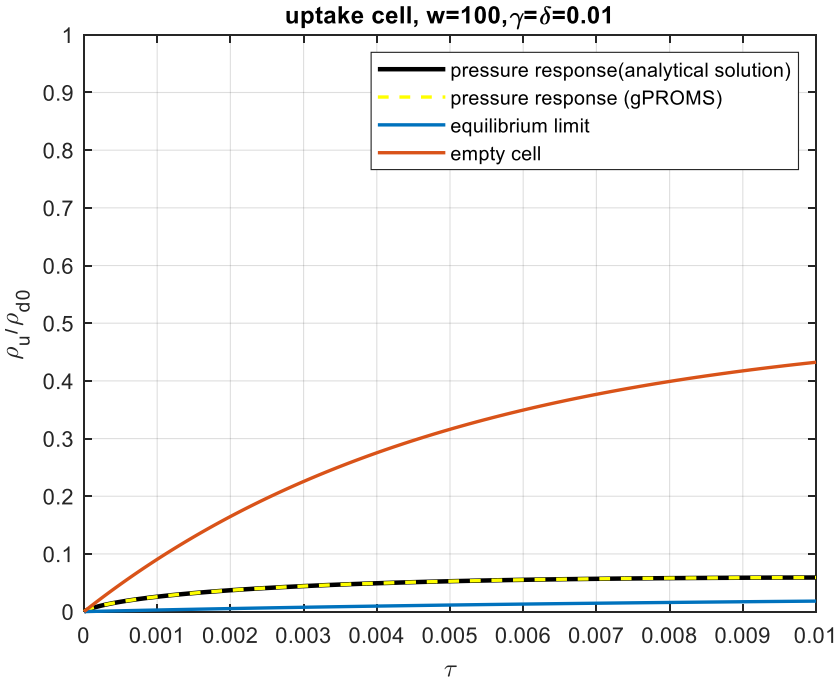

***Figure 10**: pressure response in uptake cell with ω =100*

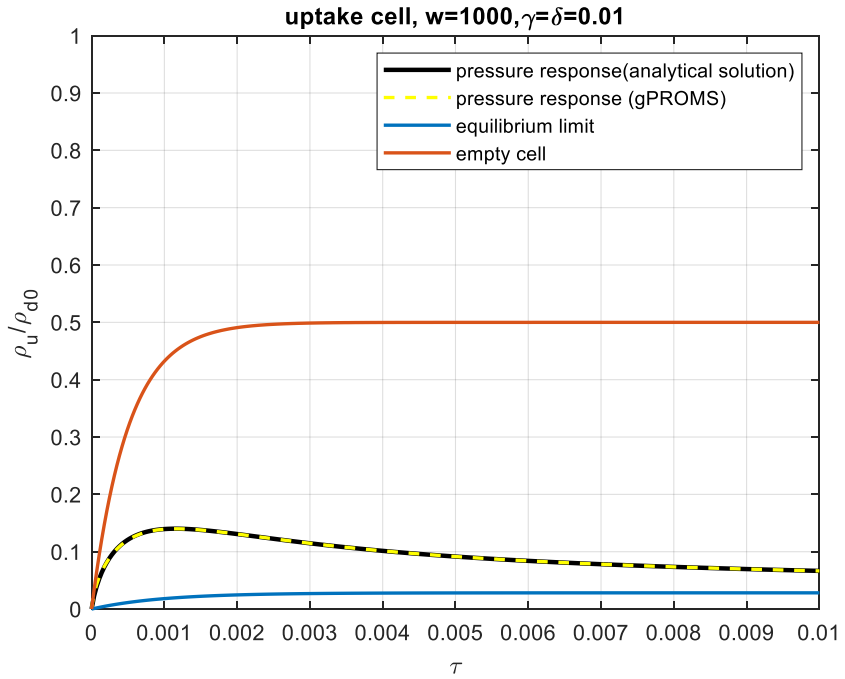

***Figure 11**: pressure response in uptake cell with ω =1000*

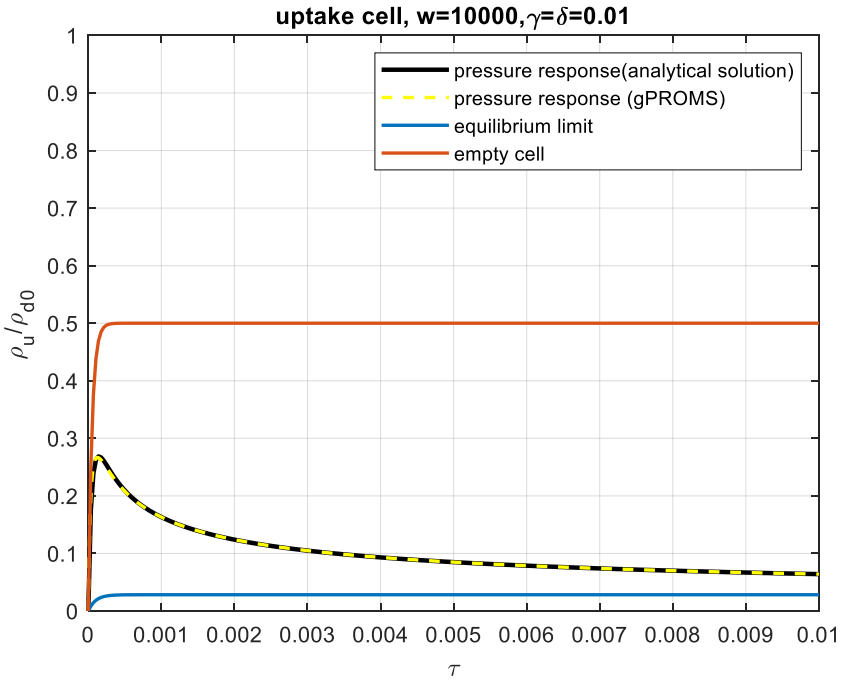

***Figure 12**: pressure response in uptake cell with ω =10000*

Analysing the Fig. 10 respect to the Fig. 11-12, when $\omega > 100$, so the conditions are far removed from equilibrium control, the pressure in the uptake cell exhibits a distinct maximum, rather than rising monotonically to its final equilibrium value. This means that the identification of this maximum in the trend of the response pressure in the uptake cell can represents a reliable indication of mass transfer.

Anyway, the results obtained show that there is an excellent agreement between the analytical solution and the mathematical model implemented.

As further validation of the model was carried out, and also in this case, was used the parameters provided by Brandani (1998). The parameters used by the author and inside the model are shown in the table below.

***Table 3**: constant parameters (Brandani, 1998)*

Volume of solid	V_s	5.33E-09	m^3
Volume of dosing cell	V_d	1.20E-04	m^3
Volume of uptake cell	V_u	8.00E-05	m^3
Temperature of dosing cell	T_d	353	K
Temperature of uptake cell	T_u	353	K
Diffusivity	D	2.00E-11	m^2/s
Radius of crystals	R_p	6.00E-05	m
Equilibrium constant	K	1.00E+07	
Valve constant	χ	1.30E-08	mol Pa^{-2} s^{-1}
Pressure in dosing cell	$P_{d,0}$	30	Pa
Pressure in uptake cell	$P_{u,0}$	20	Pa
	γ	0.0005	
	δ	0.00075	
	ω	2860	

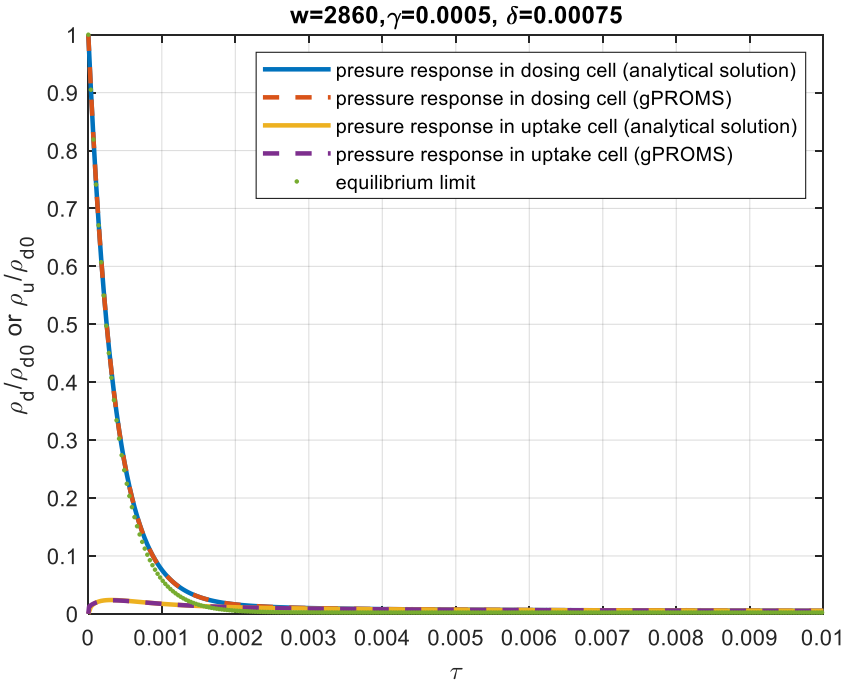

***Figure 13**: curves calculated using parameters reported in Table 1*

Pressure response for both dosing and uptake cells calculated starting from these parameters are shown in Fig. 13. It is evident how, with the value of diffusivity used, the uptake curve is basically indistinguishable from the equilibrium controlled limiting case, with the process that is practically complete in less than 1 s ($\tau = 0.05$). However, also in this case there is perfect match between the results, confirming the robustness of the mathematical model implemented in gPROMS.

3.2 Non-Isothermal case of a single-branch Volumetric system

3.2.1 Process Description & Mathematical Model

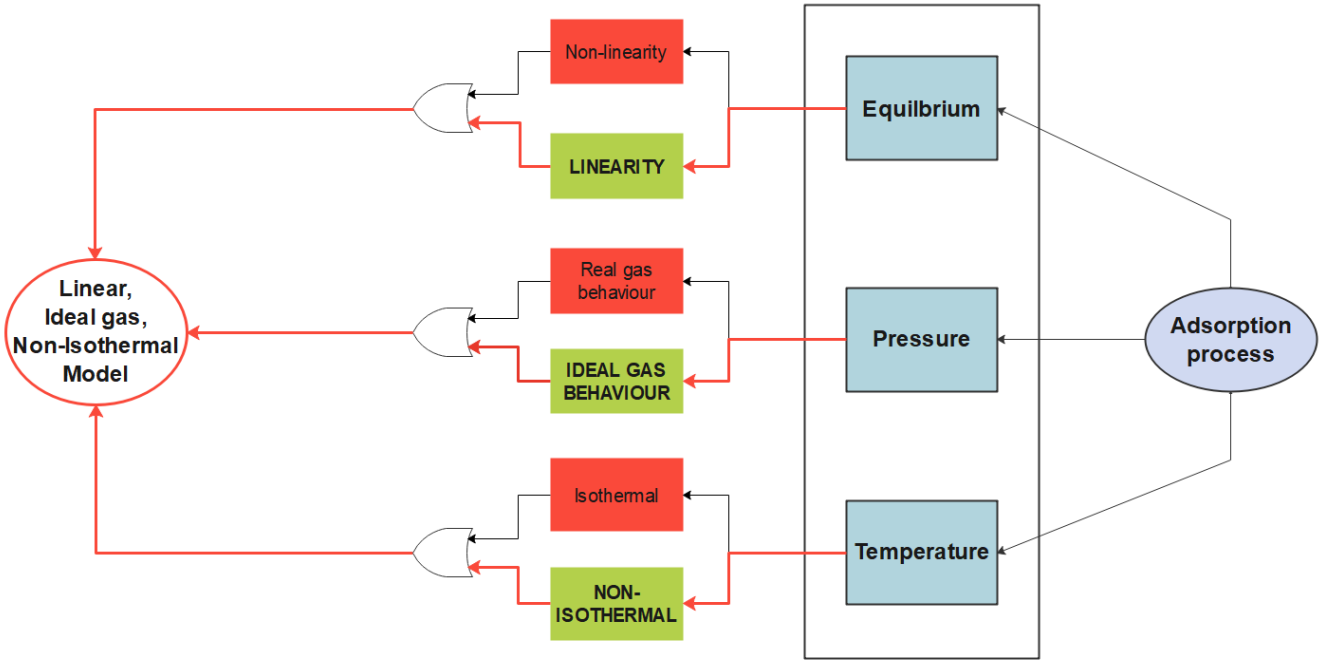

Figure 14: *Pathway map of the model*

As was saw before, the method used to study the kinetic of an adsorption system is to measure the transient adsorption curve generated when a sample of the adsorbent is exposed to a change in ambient sorbate concentration. Such curves are generally analysed according to a simple isothermal diffusion model. This approximation is valid when the diffusion is slow compared with heat transfer, but for rapidly diffusing systems, the sorption kinetics may be appreciably influenced by thermal effects (Ruthven, Lee, & Yucel, 1980). In a non-isothermal system there are two effects: the temperature dependence of the equilibrium adsorbed phase concentration at the adsorbent surface and the temperature dependence of the diffusivity. It is possible to eliminate the latter effect by reducing the size of the concentration step over which the uptake curve is measured, but the first effect is independent of step size. Heat conduction through an adsorbent particle or through an assemblage of adsorbent particles is generally much faster than heat transfer at the external surface so it is usually a good approximation to consider the particle

as essentially isothermal with all heat transfer resistance concentrated in the external film (Ruthven, 1984).

In this section is presented a non-isothermal model for spherical adsorbent particles. The assumptions of the mathematical model are the follows:

- The sample consists of an assemblage of uniform spherical particles
- Only the enthalpy term appears in the solid during the adsorption
- Heat is transferred between the solid phase and the gas phase
- Intraparticle diffusion is the only significant resistance to mass transfer
- The diffusivity is assumed constant and the equilibrium relationships are linear

So, considering these assumptions, the energy balance for the sample can be expressed as:

$$\rho_s c_{p,s} \frac{dT_s}{dt} + h_s a_s (T_s - T_U) + (-\Delta H) \frac{d\bar{q}}{dt} = 0 \qquad (3.21)$$

Where ρ_s is density of the sample, $-\Delta H$ is the heat of adsorption of the sample, $c_{p,s}$ is the specific heat capacity of the sample, T_U is the gas phase temperature, h_s is the heat transfer coefficient of solid phase, a_s is the external surface area per unit volume of the sample.

The equation above can be rewritten through the definition of two dimensionless parameters α and β. The first one represents the ratio of the time constant for diffusion and heat transfer, while the second depends on the heat of adsorption, the thermal capacity, and the temperature coefficient of the equilibrium position, and are expressed as:

$$\alpha = \frac{h_s a_s}{\rho_s c_{p,s}} \cdot \frac{1}{D/R^2}$$

$$\beta = \frac{(\Delta H)(q_\infty - q_0)}{\rho_s c_{p,s} T_0}$$

In this way the previous equation assumes the form:

$$\frac{dT_S'}{d\tau} = \alpha (T_U' - T_S') + \beta \frac{d\bar{Q}}{d\tau} \qquad (3.22)$$

Where $T_S' = \frac{T_S}{T_0}$

The energy balance around the gas phase in the uptake cell includes heat transfer to the solid phase and to the cell wall (Kye, Jae, & Won, 1994):

$$\varepsilon \rho_g c_{p,g} \frac{dT_U}{dt} + (1-\varepsilon) h_s a_s (T_U - T_s) + h_w a_{w1} (T_U - T_w) = 0 \qquad (3.23)$$

Where ρ_g is density of the gas, $c_{p,g}$ is the specific heat capacity of the gas, T_w is the temperature of the wall, h_w is the heat transfer coefficient from the gas phase to the wall, a_{w1} is the ratio of the internal surface area to the volume of the cell.

Finally, the energy balance for the cell wall, which includes the wall heat transfer to the external environment and to the gas phase inside the cell, can be expressed as follows:

$$\rho_w c_{p,w} \frac{dT_w}{dt} + h_w a_{w2} (T_w - T_U) + U_a a_a (T_w - T_\infty) = 0 \qquad (3.24)$$

Where ρ_w is cell wall density, $c_{p,w}$ is the specific heat capacity of the cell wall, U_a is the external overall heat transfer coefficient form the wall to ambient air, T_∞ is the ambient temperature, a_{w2} and a_a are the ratio of the internal surface area to the volume of the cell wall and the ratio of the logarithmic mean surface to the volume of the cell wall, respectively. In the same way it is possible to write the energy balance for the dosing cell. The energy balance for the gas has the same form saw for the one in the uptake cell neglecting the term referring to the solid:

$$\rho_g c_{p,g} \frac{dT_D}{dt} + h_w a_{w1} (T_D - T_w) = 0 \qquad (3.25)$$

$$\rho_w c_{p,w} \frac{dT_w}{dt} + h_w a_{w2} (T_w - T_D) + U_a a_a (T_w - T_\infty) = 0 \qquad (3.26)$$

Also the above equations can be written in a dimensionless form:

$$\frac{dT_U'}{d\tau} = \gamma (T_S' - T_U') + \delta (T_w' - T_U') \qquad (3.27)$$

$$\frac{dT_w'}{d\tau} = \lambda (T_U' - T_w') - \theta \left(T_w' - \frac{T_\infty}{T_0} \right) \qquad (3.28)$$

$$\frac{dT_D'}{d\tau} = \varphi(T_w' - T_D') \tag{3.29}$$

$$\frac{dT_w'}{d\tau} = \lambda(T_D' - T_w') - \theta\left(T_w' - \frac{T_\infty}{T_0}\right) \tag{3.30}$$

The different dimensionless parameters are reported in the table below.

***Table 4**: Dimensionless parameters*

SOLID	UPTAKE CELL	WALL	DOSING CELL
$\alpha = \frac{h_s a_s}{\rho_s c_{p,s}} \frac{1}{D/R^2}$	$\gamma = \frac{(1-\varepsilon)}{\varepsilon} \frac{h_s a_s}{\rho_g c_{p,g}} \cdot \frac{1}{D/R^2}$	$\lambda = \frac{h_w a_{w,2}}{\rho_w c_{p,w}} \cdot \frac{1}{D/R^2}$	$\varphi = \frac{h_w a_{w,1}}{\rho_g c_{p,g}} \cdot \frac{1}{D/R^2}$
$\beta = \frac{(\Delta H)(q_\infty - q_0)}{\rho_s c_{p,s} T_0}$	$\delta = \frac{h_w a_{w,1}}{\varepsilon \rho_g c_{p,g}} \cdot \frac{1}{D/R^2}$	$\theta = \frac{U_a a_a}{\rho_w c_{p,w}} \cdot \frac{1}{D/R^2}$	$T_D' = \frac{T_D}{T_0}$
$T_s' = \frac{T_s}{T_0}$	$T_U' = \frac{T_U}{T_0}$	$T_w' = \frac{T_w}{T_0}$	

Since the temperature of the system changes, the Henry constant also changes. The temperature dependence of it can be described with the van't Hoff equation:

$$q(R,t) - q_0 = K(T) \cdot (c(t) - c_0) \tag{3.31}$$

$$K(T) = K_0 \exp\left(-\frac{\Delta H}{R_g}\left(\frac{1}{T_s} - \frac{1}{T_{ref}}\right)\right)$$

3.2.2 Model Validation

In general physical adsorption from the gas phase is invariably exothermic, property that was determined thermodynamically. Hence, after the implementation of the above equations, during the simulation an increase in temperature of the sample should be seen, which will reach a peak and then decrease back to the equilibrium value.

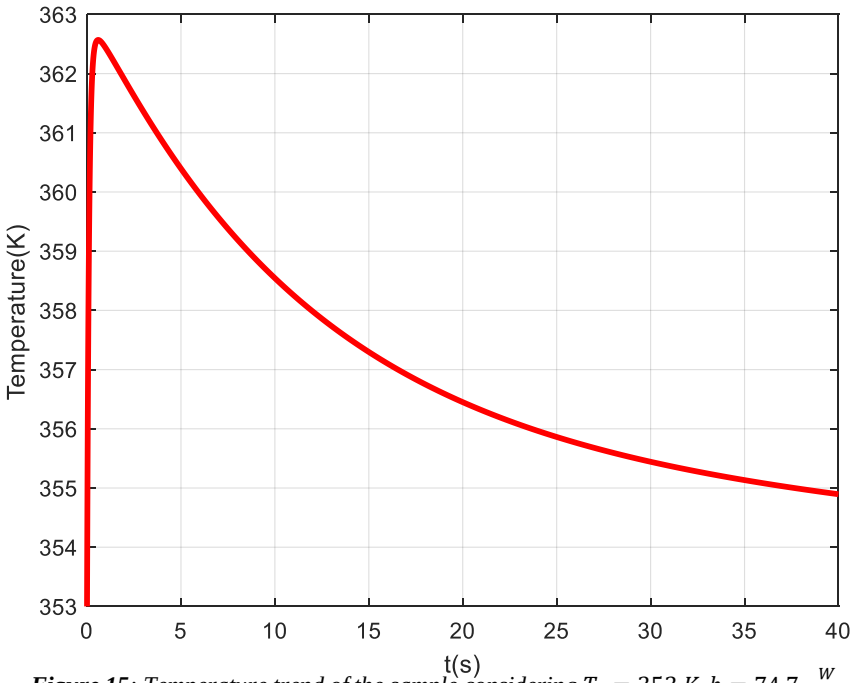

***Figure 15**: Temperature trend of the sample considering* $T_0 = 353\ K, h = 74.7\ \frac{W}{m^2 K}, \Delta H = -80\ \frac{kJ}{mol}$, $c_p = 1.2 \frac{kJ}{kg\ K}$

The general features of the reduced pressure curves are shown in Fig. 16. When diffusion is rapid (α small) the kinetics of sorption are controlled entirely by heat transfer. When heat transfer is controlling, the reduced pressure curves show a rapid initial decay followed by a slow approach to equilibrium, so the presence of a distinct break in an uptake curve could provide a useful clue that heat transfer resistance may be important.

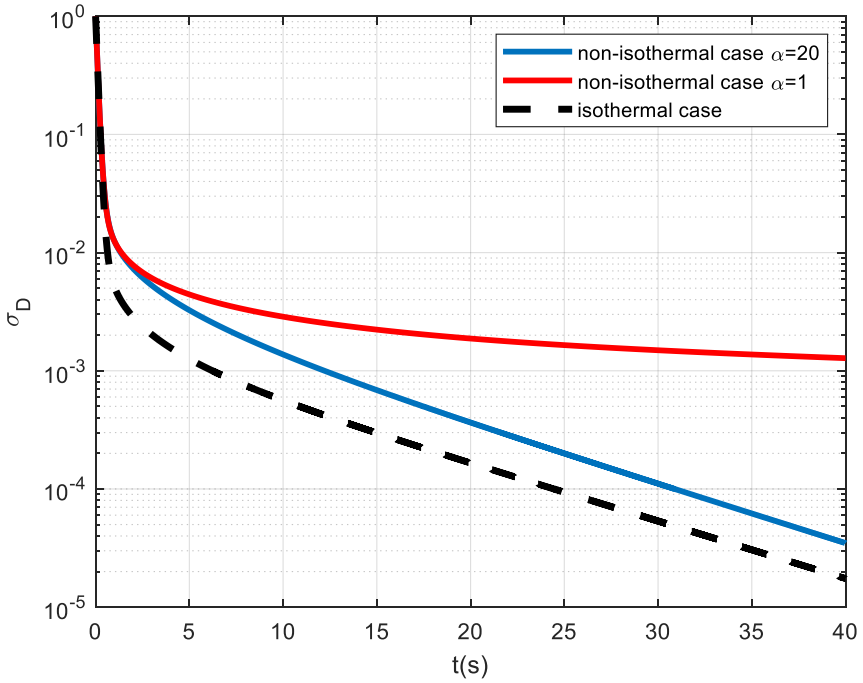

Figure 16: *uptake curves at different α, the value of β for the red and blue curves is equal to 0.03. The analysis was made considering only the temperature variation of the sample*

A verification of the reliability of the model, can be made considering the limiting case in which the system under analysis is isothermal. This particular configuration is obtained when either $\alpha \to \infty$ (infinitely heat transfer coefficient) or $\beta \to 0$ (infinitely large heat capacity). In this condition, the non-isothermal model must collapse on the isothermal case. The analysis was made comparing the variation of the reduced pressure in the two different cases.

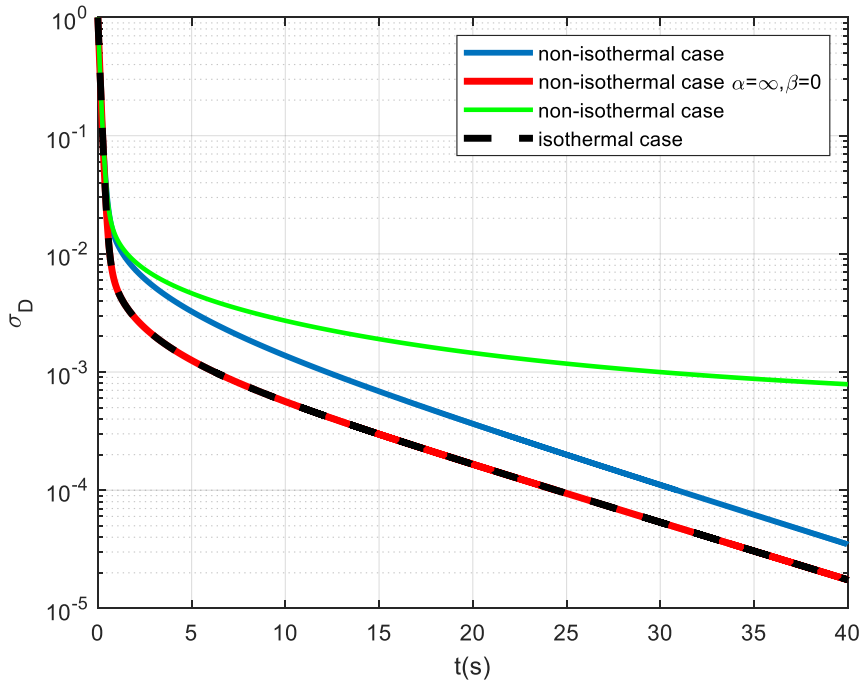

***Figure 17**: uptake curve of the two models. For the non-isothermal case the data used were* $h_s = 74.7\ \frac{W}{m^2 K}, \Delta H = -80\ \frac{kJ}{mol}, c_{p,s} = 1.2 \frac{kJ}{kg\ K}$. *The blue line considers only the temperature variation of the solid*

As it is possible to observe form the graph above the trend of the reduced pressure of the non-isothermal model overlaps the one of the isothermal case as had been predicted before. Furthermore, since the exothermical nature of the adsorption process, the production of heat leads to an inevitable reduction of the substance adsorbed by the material, behaviour that is clearly explained from the blue and green curves.

3.2.3 Case study: effect of stainless steel beads on the thermal behaviour of the sample

During an experimental analysis in order to ensure isothermal conditions beads of different materials are added to the uptake cell to increase the thermal mass of the sample (usually are used stainless steel beads). Indeed, if the experiment is performed in vacuum conditions the primary contribution to heat transfer is through radiative heat transfer. The presence of the beads reduces significantly the adiabatic temperature rise and improves the heat transfer kinetics providing direct contact with the adsorbent beads and thus increasing the overall heat transfer surface. Furthermore, the adding of inert metal beads have the additional benefit of reducing the volume in the uptake cell and increase the sensitivity of the experiment (Wang, Mangano, Brandani, & Ruthven, 2020).

As an example, was considered the adsorption of carbon dioxide on 13X zeolite beads. Several studies have indicated zeolite 13X as one of the best adsorbents available commercially for post-combustion applications. For this reason, is very often used as a benchmark material for the comparison with other candidates for CO_2 separation processes (Hu, Mangano, Friedrich, Ahn, & Brandani, 2013).

To ensure linear conditions the analysis was performed with small pressure steps, a further verification of the linearity condition can be made carried out also a desorption analysis, indeed under non-linear conditions adsorption and desorption curves will be different (see Section 3.3) (Brandani, Brandani, Mangano, & Pullumbi, 2019).

The experiment consists in injecting a certain amount of CO_2 in the uptake cell, at constant temperature of 10 °C, the adsorbent is present in the form of spherical beads with an average radius of 0.98 mm. The value of diffusivity and Henry constant are obtained through kinetic analysis carried out with a Quantachrome Autosorb-iQ^{TM} (Hu, Mangano, Friedrich, Ahn, & Brandani, 2013).

***Table 5**: parameters used in the simulation (Hu, Mangano, Friedrich, Ahn, & Brandani, 2013)*

Volume of solid	V_s	3.94E-09	m^3
Initial temperature	T_0	283.15	K
Diffusivity	D	5.20E-10	m^2/s
Mass of sample	m_s	38	mg
Radius	R	0.98	mm
Equilibrium constant	K	11679	
Valve constant	chi	2.06E-08	mol Pa^{-2} s^{-1}
Pressure in dosing cell	$P_{d,0}$	300	Pa
Pressure in uptake cell	$P_{u,0}$	52.5	Pa
$ha/(\rho_s c_{ps})$		0.04	s^{-1}
α		74.07	
β		5.5	

As first instance, the simulation was done considering only the presence of the sample. Then, was simulated the insertion of 1800 mg of 1/16'' stainless steel beads with a density of 7817 $\frac{kg}{m^3}$ that, as was already said, ensure isothermal condition inside the system.

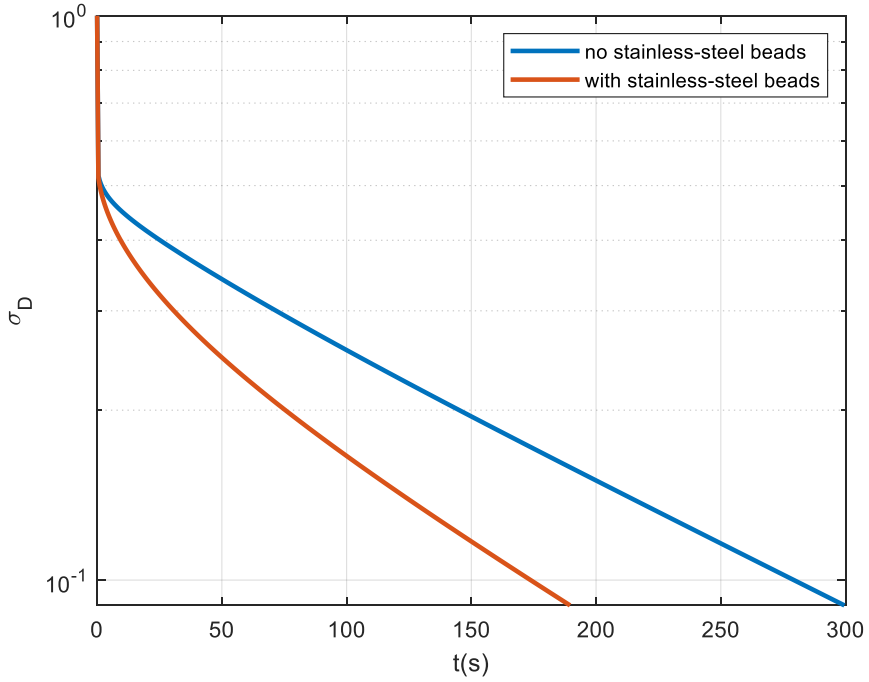

***Figure 18**: volumetric uptake curves*

The high value of the parameter α indicates that the system is essentially controlled by the diffusion mechanism, anyway there is also a small contribution from the heat generated during the adsorption. In other words, a large value of α implied that the heat generated during adsorption is transferred to the surrounding environment rather than increasing the temperature

of the adsorbent (Park, Ju, Park, & Lee, 2016). At higher concentrations of the gas the contribution of the heat transfer limitations is more significant, indeed, even if the adsorption curves exhibit a very fast initial uptake, in the long-time region the adsorption rate, for the non-isothermal process, is slower respect the isothermal process.

Such behaviour is typical of a heat limited process in which the kinetics are initially fast, but then the slow decay is related to the dissipation of the heat generated by adsorption, resulting in additional slow uptake as the particle cools (Hu, Mangano, Friedrich, Ahn, & Brandani, 2013).

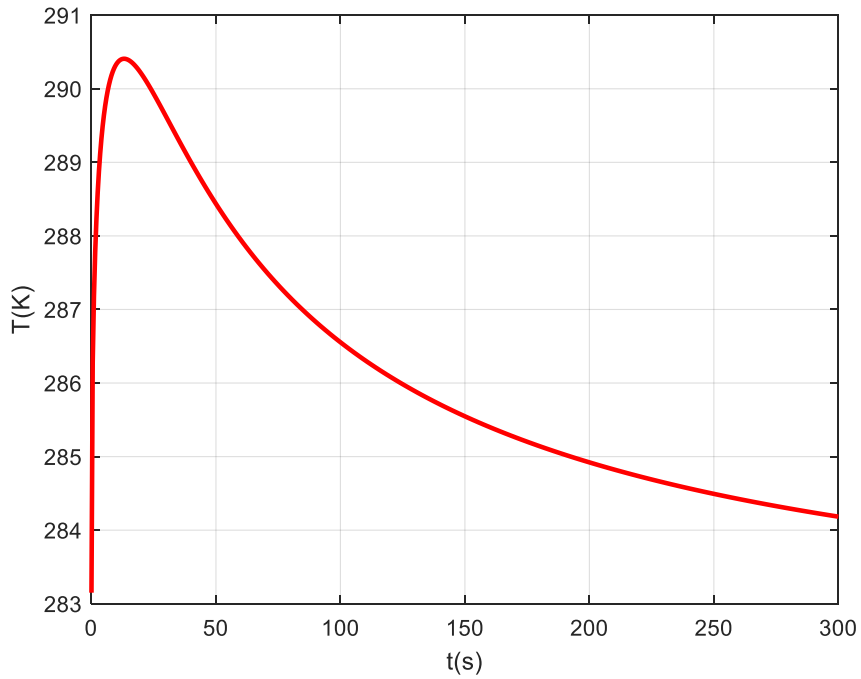

***Figure 19**: Temperature trend of the sample without stainless-steel beads*

3.3 Isothermal and non-linear case of a single-branch Volumetric system

3.3.1 Process Description & Mathematical Model

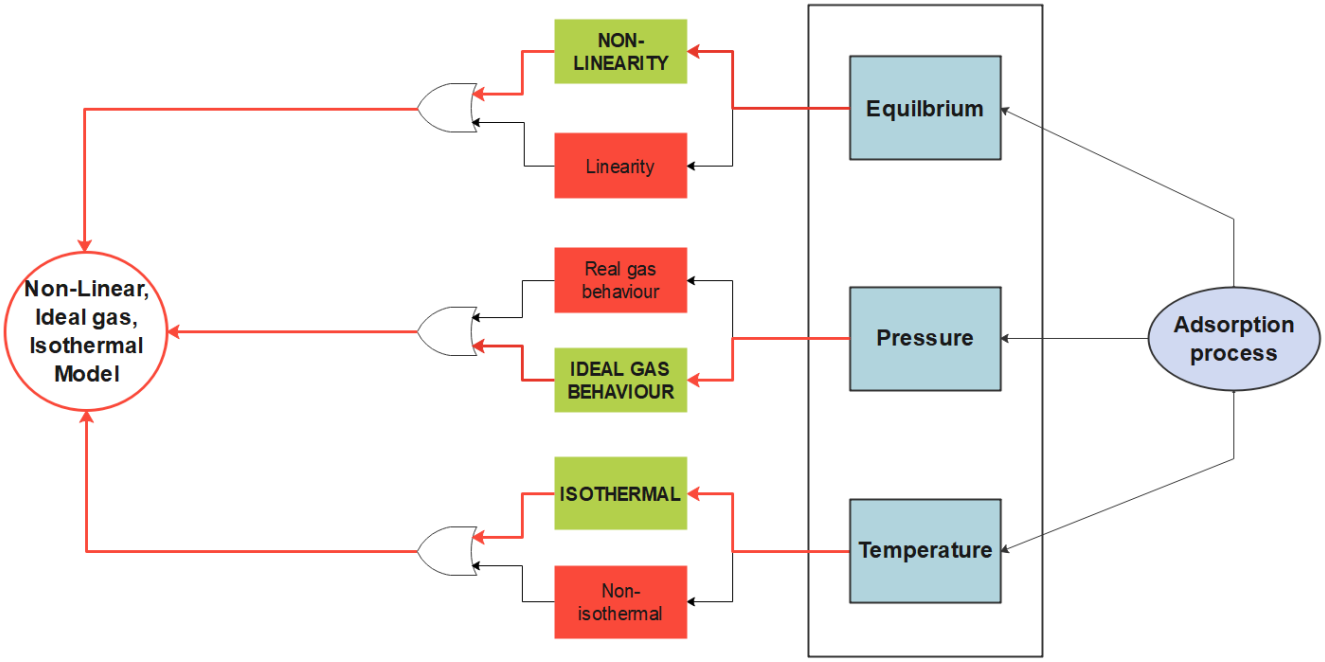

***Figure 20**: Pathway map of the model*

If the change in concentration over which the uptake curve is measured is large, the effect of non-linearity of the equilibrium isotherm must be considered (Ruthven, 1984). The most important effect of the non-linearity is an evident difference between adsorption and desorption steps, with the adsorption that is faster than the desorption (Wang, Mangano, Brandani, & Ruthven, 2020). A typical case in which this behaviour occurs is when strongly adsorbed species are considered.

The nonlinear equilibrium is taken into account considering Langmuir adsorption isotherm. Assuming a spherical particle and the diffusivity to be concentration dependent, the mass balance is:

$$\frac{\partial q}{\partial t} = \frac{1}{r^2}\frac{\partial}{\partial r}\left(D(q)\cdot r^2\frac{\partial q}{\partial r}\right) \tag{3.32}$$

and

$$\frac{\partial \bar{q}}{\partial t} = \frac{3}{R}\left(D(q) \cdot \frac{\partial q}{\partial r}\right)_{r=R} \tag{3.33}$$

For the boundary condition was assumed Langmuir equilibrium at the surface and the symmetry condition.

The basic assumptions on which the Langmuir model is based are (Martinez-Vertel, et al., 2018):

- The adsorbing gas molecules adsorb into an immobile state
- The adsorbate organizes in the form of a monolayer on the surface of the adsorbent
- There are no interactions between adsorbate molecules on adjacent sites
- The solid surface has a certain amount of positions for adsorption and each position is equivalent in terms of energy levels. Therefore, there is not any preference to occupy a specific place

$$q(R,t) = q_s \frac{bc}{1+bc} \tag{3.34}$$

Where q_s is the concentration of saturation of the adsorbate and b is the Langmuir parameter.

Final assumption is that the concentration dependence of the diffusivity can be described according to Darken's equation (Karger & Ruthven , 1992) which for the Langmuir isotherm yields:

$$D(q) = D_0 \frac{d \ln P_u}{d \ln q} = D_0 \frac{1}{1 - {}^{q}/_{q_s}} \tag{3.35}$$

Where D_0 is the intracrystalline diffusivity and $\frac{d \ln P_u}{d \ln q}$ is the Darken correction factor.

The fractional uptake is a function of the dimensionless time variable and the size or nonlinearity, measured by the parameter $\lambda = \frac{q_\infty}{q_s}$. Consequently, the Darken's equation can be rewritten as function of the parameter λ. At small values of λ the system approaches linearity,

so adsorption and desorption curves are mirror images and the uptake rate is independent of step size but for larger concentration steps the rate becomes depend on step size and adsorption is much faster than desorption (Garg & Ruthven, 1971):

$$D(q) = D_0 \frac{d \ln P_u}{d \ln q} = D_0 \frac{1}{1 - {}^{q}/_{q_s}} = \frac{D_0}{1 - \lambda \frac{q}{q_\infty}} \tag{3.36}$$

The Darken correction factor is a thermodynamic coefficient that is important in the determination of the corrected diffusivity in micropores. The definition is given by:

$$\frac{d \ln P_u}{d \ln q} = \frac{q/P_u}{dq/dP_u} = \frac{q/c}{dq/dc} \tag{3.37}$$

Eq. 3.37 indicates that in order to calculate the Darken correction factor it is necessary to have an accurate value of the secant of the isotherm, q/P_u, and the slope of the isotherm, dq/dP_u (Brandani & Hu, 2011). Considering the Langmuir isotherm, the value of the Darken correction factor is 1 in the Henry law region, while it is infinity at saturation.

In general, the single-site Langmuir equation cannot sufficiently describe a large number of real gas-solid adsorption systems. For heterogeneous surfaces, which are the most common, the adsorption energy at each site will vary, depending on the local chemistry and structure. The most favourable sites will be filled first, followed by the less favourable sites. In order to address heterogeneous adsorbents, the most simplified case is where only two different adsorption sites are available. Each site can be modelled by a separate equilibrium constant, b_1 and b_2. Thus, the dual-site Langmuir equation can be written in the following form (Tang, Ripepi, Stadie, Yu, & Hall, 2016):

$$q(R,t) = q_{s1} \frac{b_1 c}{1 + b_1 c} + q_{s2} \frac{b_2 c}{1 + b_2 c} \tag{3.38}$$

3.3.2 Model Validation

As first instance, the analysis was carried out considering the single-site Langmuir equation, and the Langmuir parameter was calculated as $K = b \cdot q_s$ choosing an arbitrary value of q_s and using the Henry constant of the linear case (Section 3.1.2, Table 3). Then, were compared the isotherm curves for the Henry and Langmuir models. What should be seen is that in the low concentration region the two curves overlap, due to the correspondence of the models, since for Langmuir, when $bc \ll 1 \rightarrow \frac{q}{q_s} \approx bc$; while at high value of c should be the saturation of the material, and therefore the presence of a plateau in correspondence of q_s.

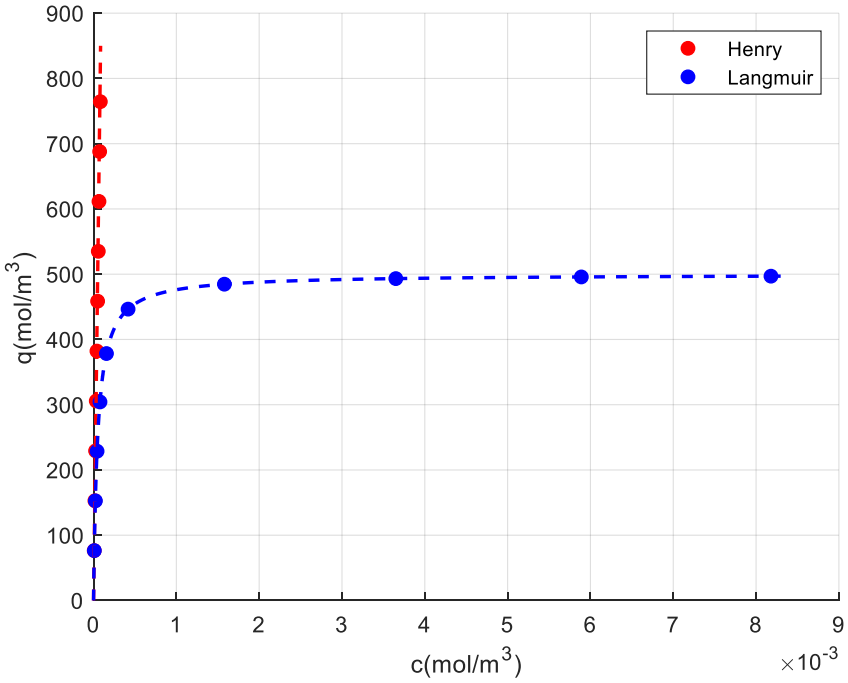

***Figure 21**: Adsorption curves of the two models. For the analysis was chosen a value of q_s equal to $500\, mol/m^3$*

Fig. 21 shows the trends of the two models, the qualitative behaviour described before is confirmed.

3.3.3 Case study: effect of pressure step on the kinetic of the system

To ensure linearity conditions, adsorption experiments are performed with small pressure steps. It is also important to measure both the adsorption and desorption response as this provides a simple check on system linearity.

A typical error made during volumetric analysis, especially when the kinetic is studied, is increasing the pressure step. Generally, it is done in order to record a better signal by the system, because a higher quantity of gas is adsorbed. This leads, not only to the creation of non-isothermal condition, but also to the fact that the isotherm is no longer linear. Usually, all these effects are neglected so the data are analysed using an isothermal and linear model (Wang, Mangano, Brandani, & Ruthven, 2020).

In order to study the effect of the pressure step, two different case are analysed, in the first one is considered a small pressure step between the dosing and the uptake cell, while in the second one the pressure step is increased imposing vacuum condition in the uptake cell; the simulation was done considering the adsorption of CO_2 in CPO-27-Ni beads.

Metal organic frameworks (MOFs) are a new class of materials, which have a high surface area and a large pore volume, one of the widely studied MOFs is the CPO-27-Ni. This material possesses open metal sites, which can interact with different gas molecules and a potential application for this material is to capture and concentrate CO_2 from post-combustion flue gas streams.

Different published studies have shown that this material have a very high CO_2 capacity comparable to that of Zeolite 13 (the current benchmark material for CO_2 capture applications) (Krishnamurthy, Blom, Ferrari, & Brandani, 2019).

The simulation was carried out a temperature of 35 °C and, also in this case, the adsorbent is present in the form of spherical beads with an average radius of 1.6 mm. The value of diffusivity is obtained through volumetric experiments carried out with a Quantachrome Autosorb-iQ™.

The analysis was made adopting the dual-site Langmuir isotherm expressed as function of the pressure in the uptake cell:

$$q(R,t) = q_{s1}\frac{b_{0,1}e^{-\frac{\Delta H_1}{RT}}P_u}{1+b_{0,1}e^{-\frac{\Delta H_1}{RT}}P_u} + q_{s2}\frac{b_{0,2}e^{-\frac{\Delta H_2}{RT}}P_u}{1+b_{0,2}e^{-\frac{\Delta H_2}{RT}}P_u} \tag{3.39}$$

***Table 6**: Parameters used in the simulation (Krishnamurthy, Blom, Ferrari, & Brandani, 2019)*

Volume of solid	V_s	1.71E-08	m^3
Initial temperature	T_0	308	K
Diffusivity	D	3.07E-08	m^2/s
Radius	R	1.6	mm
Valve constant	χ	1.41E-06	mol Pa^{-2} s^{-1}
Equilibrium constant	K	112.5	
Pressure in dosing cell	$P_{d,0}$	21770	Pa
Pressure in uptake cell	$P_{u,0}$	19920	Pa
$q_{s,1}$		3284.211	mol/m^3
$b_{0,1}$		1.50E-11	Pa^{-1}
ΔH_1		-39.9	kJ/mol
$q_{s,2}$		3251.462	mol/m^3
$b_{0,2}$		9.00E-11	Pa^{-1}
ΔH_2		-23.6	kJ/mol

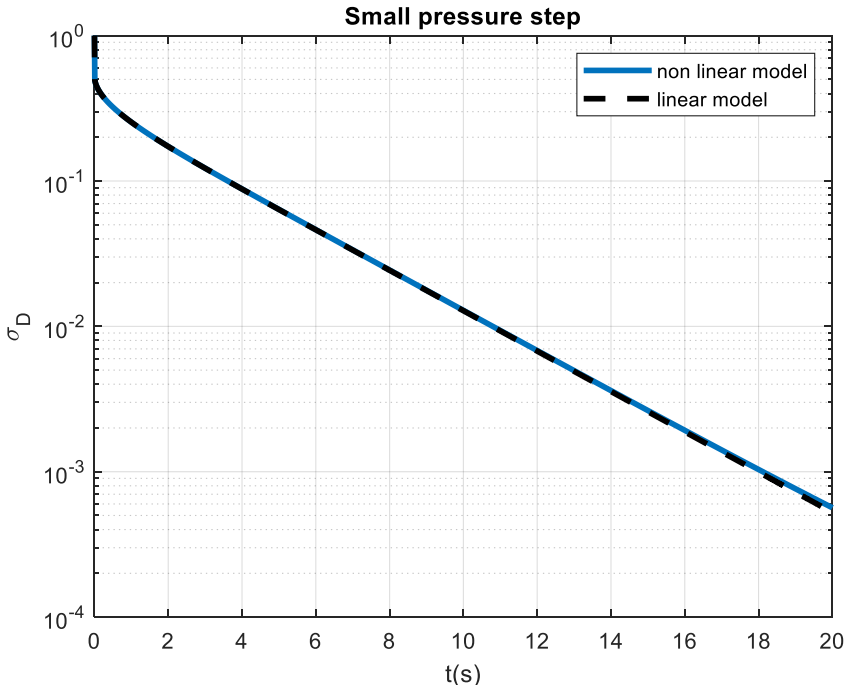

***Figure 22**: uptake curves for a small pressure step*

From the Fig. 22 it is possible to observe how the trend of the reduced pressure of the linear and non-linear model overlap.

This because, even if with the pressure used the system is far from the region where the isotherm can be considered linear (which is valid only for pressure values very low), the use of a small pressure step allows to approximate that part of the isotherm with a straight segment.

Behaviour that is not present in the other case, represented by the Fig. 23, where there is a high discrepancy between the results obtained with the linear and non-linear model.

So, in this sense is very important, before any type of experiments, choose the right assumptions in order to avoid the creation of erroneous results.

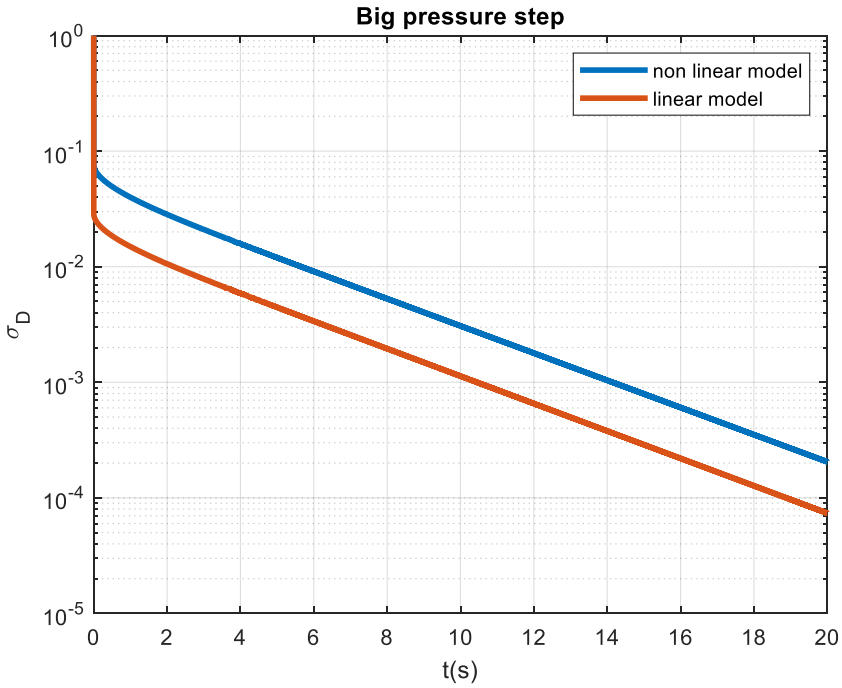

***Figure 23**: uptake curves for a big pressure step*

3.4 Non-Isothermal and non-linear case of a single-branch Volumetric system

3.4.1 Process Description & Mathematical Model

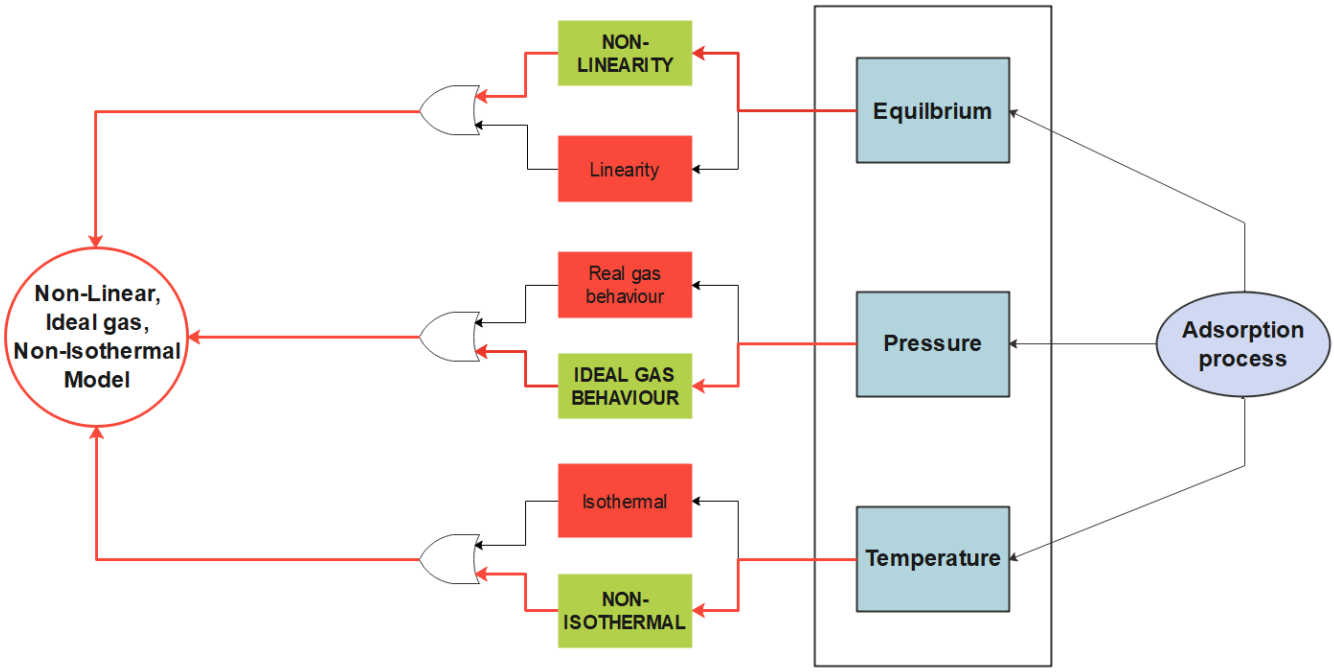

***Figure 24**: Pathway map of the model*

In this section is studied the dependence of the Langmuir parameter as function of the temperature. Now, the Langmuir equation becomes:

$$q(R,t) = q_s \frac{b(T) \cdot c}{1 + b(T) \cdot c} \tag{3.40}$$

Also in this case the parameter $b(T)$ can be expressed with the van't Hoff equation:

$$b(T) = b_0 \exp\left(-\frac{\Delta H}{R_g T_s}\right)$$

Where b_0 is the temperature-dependent constant. The Langmuir constant is affected by the physical properties of the adsorbent gas, adsorbate-adsorbent gas interaction and the status of the sorption system. In general, $b(T)$ should decrease with increasing temperature according to the van't Hoff equation (Tang & Ripepi, 2016). For the energy balance were used the same equations saw in the Chapter 3.2.

The isosteric heat for the Langmuir isotherm equation is expressed from the following formula (Do, 1998):

$$(-\Delta H) = \frac{\sum_{i=1}^{N} q_{s,i} \frac{b_i \Delta H_i}{(1+b_i P_u)^2}}{\sum_{i=1}^{N} q_{s,i} \frac{b_i}{(1+b_i P_u)^2}} \tag{3.41}$$

3.4.2 Model Validation

As has already been demonstrated for the linear case, since the exothermic behaviour of the adsorption process, the production of heat leads to a reduction in the quantity adsorbed by the sample. This mechanism is represented graphically with the reduced pressure curve shifted upwards with respect to the curve of the isothermal model. A second proof of the reliability of the model was obtained through the achievement of exothermicity when either $\alpha \to \infty$ or $\beta \to 0$.

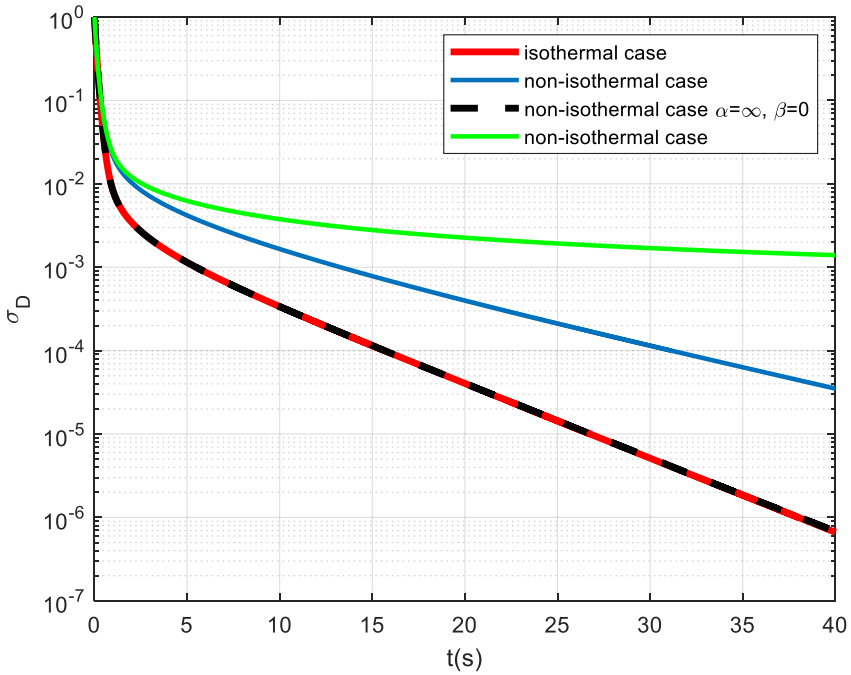

***Figure 25**: uptake curve of the two models. For the non-isothermal case the data used were $h_s = 74.7\ \frac{W}{m^2 K}, \Delta H = -80\ \frac{kJ}{mol}, c_{p,s} = 1.2\ \frac{kJ}{kg\ K}$. The blue line considers only the temperature variation of the solid*

3.4.3 Case study: adsorption kinetics of CO_2 and N_2 on 13X zeolite

As was already showed the adsorption process represents a promise technology for the CO_2 capture from flue gases associated with combustion and chemical processes, due to possessing inherently low energy consumption.

Furthermore, adsorption processes have been studied for the recovery of methane from natural gas, since the high concentration of other compounds such as N_2 and CO_2 (Park, Ju, Park, & Lee, 2016).

In this sense are studied the adsorption kinetics of carbon dioxide and nitrogen on 13X zeolite at a temperature of 20 °C, the adsorbent is present in the form of spherical beads with an average radius of 1.6 mm. The simulation was carried out considering non-isothermal condition, while was assumed the single site Langmuir relationship in order to study the equilibrium of the process, expressed as function of pressure:

$$q(R,t) = q_s \frac{b(T) \cdot P_u}{1 + b(T) \cdot P_u} \tag{3.42}$$

***Table 7**: Parameters used in the simulations (Park, Ju, Park, & Lee, 2016)*

CO_2				N_2			
Volume of solid	V_s	1.71E-08	m^3	**Volume of solid**	V_s	1.71E-08	m^3
Initial temperature	T_0	293	K	**Initial temperature**	T_0	293	K
Diffusivity	D	8.45E-09	m^2/s	**Diffusivity**	D	2.61E-07	m^2/s
Radius	R	1.6	mm	**Radius**	R	1.6	mm
Pressure in dosing cell	$P_{d,0}$	87.33	kPa	**Pressure in dosing cell**	$P_{d,0}$	84.56	kPa
Pressure in uptake cell	$P_{u,0}$	77.79	kPa	**Pressure in uptake cell**	$P_{u,0}$	78.86	kPa
Initial adsorbed conc.	q_0	7246.4	mol/m^3	**Initial adsorbed conc.**	q_0	446.4	mol/m^3
$ha/(\rho_s c_{ps})$		0.012	s^{-1}	**$ha/(\rho_s c_{ps})$**		0.022	s^{-1}
α		3.63		**α**		0.21	
β		0.606		**β**		0.236	
q_s		8545.6	mol/m^3	**q_s**		5052.8	mol/m^3
b_0		1.78E-07	kPa^{-1}	**b_0**		7.21E-07	kPa^{-1}
ΔH		-33.022	kJ/mol	**ΔH**		-18.077	kJ/mol

As was stated in Chapter 3.2, the diffusional time constant is affected by the two parameters of the overall heat transfer coefficient ratio (α) and the heat of adsorption ratio (β). In this case, the small value of α implied that heat generation is concentrated during the initial part of uptake

due to the rapid uptake of molecules. Therefore, the temperature increased during adsorption, precluding adsorption on the surface. So, when the adsorbate has a strong temperature dependence, the uptake curve deviates from the isothermal model, resulting in a heat transfer-controlled system.

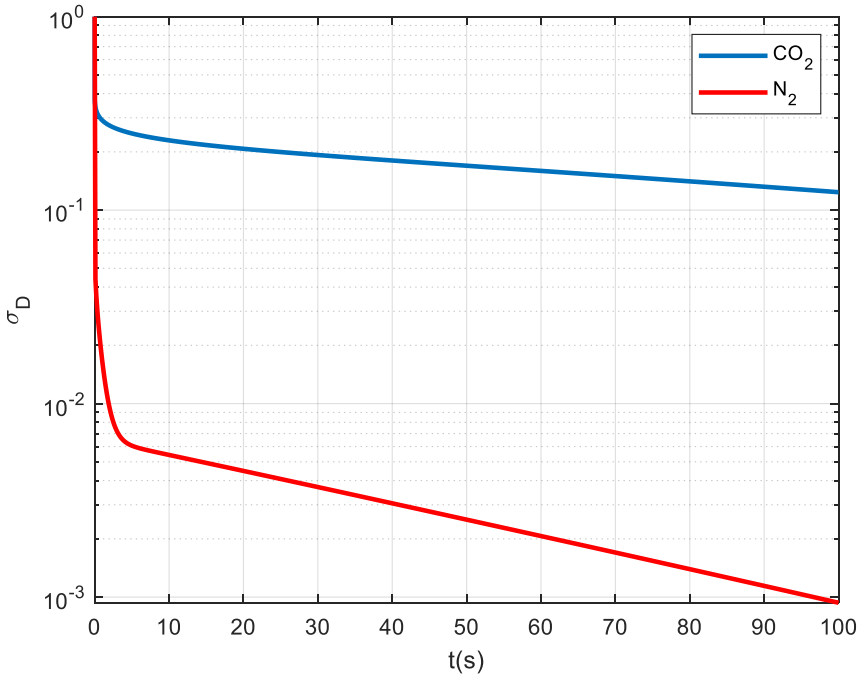

***Figure 26**: uptake curves of the compounds*

For the case under analysis, the carbon dioxide yielded an α value of 3.63, while for the nitrogen it is equal to 0.21. Although, the relative heat transfer rate for the CO_2 is higher than that of the N_2; a big value of the isosteric heat of adsorption, which is approximately 2 times higher, generates high thermal resistance during CO_2 adsorption and cause a slow CO_2 adsorption on surfaces.

Indeed, it is possible to observe that the adsorption rate of nitrogen is greater respect the one of carbon dioxide, and this is due to the different diffusivity which characterize the two substances. In particular, is evident how the curve of nitrogen presents a rapid inflection after 5 s. This behaviour should not surprise, in fact, the high value of the heat of adsorption of CO_2 is an index of high affinity between the adsorbent/adsorbate, therefore this means that, in the pressure

range considered, for carbon dioxide the system is close to saturation, and this is also evident from the value of q_0. Experimental analyses carried out with nitrogen can be made more easily, indeed with this substance, it is possible to use bigger pressure step, or higher quantity of adsorbent, because the quantity of substance adsorbed, and the heat produced is generally low. This latter aspect is well explained also from the trend reported below related to the temperature variation, where for the nitrogen, the maximum value reached is equal to 297.5 K, while for the carbon dioxide the value settles to 350 K.

The observed temperature response curves are in both cases of the expected form, they show a rapid initial rise followed by a slow return to the equilibrium temperature.

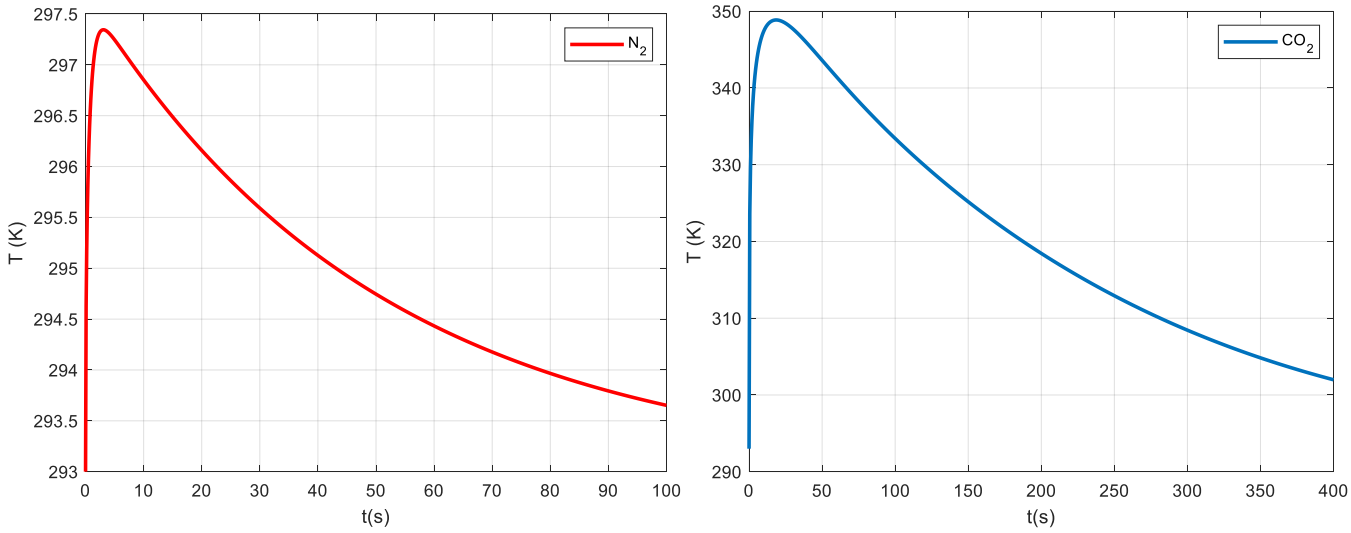

***Figure 27**: temperature behaviour for the two compounds*

3.5 Real gas behaviour case for a single-branch Volumetric system

3.5.1 Process Description & Mathematical Model

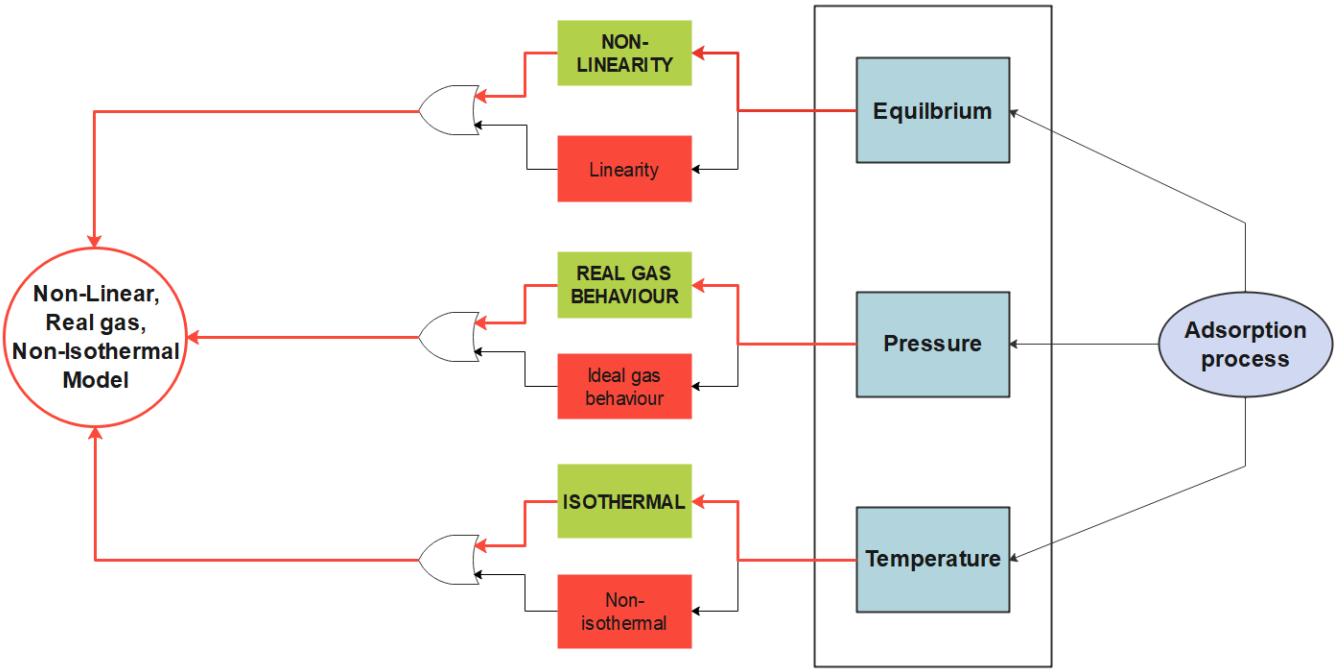

***Figure 28**: Pathway map of the model*

During the last decades, interest in high-pressure adsorption has increased in order to find technological solutions for gas storage and gas separation devices for finding methods to solve future environmental problems. This includes gas storage devices for new propulsion methods (H_2 - storage) as well as possibilities for underground CO_2 - sequestration and machines for separating different gas and vapor mixtures.

The ideal law gas describes the macroscopic state of a three-dimensional gas of non-interacting, volume less point particles. It is satisfactory for describing common gases at low pressures and high temperatures, but ineffective for real gases over a wide temperature and pressure regime (Nakhli, et al., 2014). A better approximation was determined by van der Waals, combining two important observations:

- The gas molecules or atoms have a finite volume that cannot be occupied by other molecules or atoms: this means that the volume available is not the total volume but has to be decreased by the fraction of volume occupied by each molecule

- The gas molecules interact each other causing a net attraction force on molecules at the outer surface of the system: the pressure exerted by the system on the outside wall is lower than that of ideal gas due to the molecules interactions

Considering these assumptions, the van der Waals equation of state is expressed as:

$$\left(P_u + \frac{a}{\tilde{V}_u^2}\right) \cdot \left(\tilde{V}_u - b\right) = RT_u \tag{3.43}$$

Where a and b represent the cohesion pressure and the co-volume of the adsorbate molecule, respectively. These two parameters can be calculated knowing the critical temperature (T_C) and pressure (P_C) of the substance:

$$b = \frac{RT_C}{8P_C} \quad a = \frac{27(RT_C)^2}{64P_C}$$

The Eq. 3.43 can be rewritten as a polynomial of third orders as function of the compressibility factor Z, which is a parameter that define the departure of a gas or substance behaviour from that of ideal gas:

$$Z^3 - \left(1 + \frac{bP_u}{RT_u}\right)Z^2 + \frac{aP_u}{(RT_u)^2}Z - \left(\frac{aP}{(RT_u)^2} \cdot \frac{bP_u}{RT_u}\right) = 0 \tag{3.44}$$

The Peng-Robinson equation of state is widely used for calculating the thermodynamic properties of both pure fluids and fluid mixtures. The Peng-Robinson equation offers algebraic simplicity and generality since it requires minimal data.

Only the critical temperature and pressure, and the acentric factor (ω) are needed to determine the properties for a pure fluid. In case in which a non-ideal mixture is considered, in addition are needed binary interaction parameters to determine the properties.

The Peng-Robinson equation is:

$$P_u = \frac{RT_u}{\left(\tilde{V}_u - b\right)} - \frac{a(T,\omega)}{\tilde{V}_u^2 + 2b\tilde{V}_u - b^2} \tag{3.45}$$

Where $a(T,\omega)$ is a fluid-specific constant that depends on temperature and b is a fluid-specific constant and are expressed as:

$$a(T,\omega) = 0.45724\frac{R^2T_C^2}{P_C}\alpha(T,\omega) \tag{3.46}$$

$$b = 0.07780\frac{RT_C}{P_C} \tag{3.47}$$

$$\alpha(T,\omega) = [1 + (0.37464 + 1.54226\omega - 0.26992\omega^2)(1 - \sqrt{T_r})]^2 \tag{3.48}$$

The Peng-Robinson equation can be rewritten in terms of the dimensionless compressibility factor as:

$$Z^3 - (1-B)Z^2 + (A - 3B^2 - 2B)Z - (AB - B^2 - B^3) = 0 \tag{3.49}$$

Where

$$A = \frac{aP_u}{R^2T_u^2} \quad B = \frac{bP_u}{RT_u}$$

In order to take into account the increase or decrease of the real gas temperature due to its expansion or compression the Joule-Thomson coefficient was calculated.

The rate of change of temperature with respect to pressure in an isoenthalpic process is defined as:

$$\mu_{JT} = \left(\frac{\partial T}{\partial P}\right)_H \tag{3.50}$$

A gas obeying van der Waals equation the expression of the Joule-Thomson coefficient becomes (Gans, 1993):

$$\mu_{JT} = \left(\frac{\partial T}{\partial P}\right)_H = \frac{\frac{2a}{RT} - b}{\tilde{c}_p} \tag{3.51}$$

Where a and b are the van der Waals constants and $\tilde{c}_p$ molar heat capacity of the gas.

If the Peng-Robinson equation is considered the Joule-Thomson coefficient can be expressed as a function of the compressibility factor (Tarom, Hossain, & Rohi, 2017):

$$\mu_{JT} = \frac{1}{\tilde{c}_p}\left[\frac{T}{Zc}\left(\frac{\partial Z}{\partial T}\right)\right] \tag{3.52}$$

$$\left(\frac{\partial Z}{\partial T}\right) = \frac{\left(\frac{\partial A}{\partial T}\right)(B - Z) + \left(\frac{\partial B}{\partial T}\right)(6BZ + 2Z - 3B^2 - 2B + A - Z^2)}{3Z^2 + 2(B - 1)Z + (A - 2B - 3B^2)}$$

3.5.2 Model Validation

Ideal gas is assumed to consist of molecules which have negligible volume, and that the collisions between the molecules are rare and elastic. As was already said, in high-pressure environment and especially if temperature is low, the deviation from the ideal gas behaviour is big.

This is because in high-pressure environment the volume occupied by the gas molecules is increasingly important (higher density). On the other hand, in low-temperature environment the relative portion of the molecule's kinetic energy (which is highly dependent from the temperature) is lower compared to the inter-molecule forces acting between real molecules (Kaario, Nuutinen, Lehto, & Larmi, 2010).

The compressibility factor Z is expressed as:

$$Z = \frac{P\tilde{V}}{RT} \tag{3.53}$$

For an ideal gas the compressibility factor is $Z = 1$. The value of Z generally increases with pressure and decreases with temperature. This allows repulsive forces between molecules to have a noticeable effect, making the concentration of the real gas lower that the one of the corresponding ideal gas, which causes Z to exceed one.

Instead, when pressures are lower, the molecules are free to move; in this case attractive forces dominate, making $Z < 1$. In general, the closer the gas is to its critical point, the more Z deviates from the ideal case.

A comparative analysis was made in order to verify the reliability of the equations of state implemented inside the model. In particular was studied the behaviour of the carbon dioxide in a hypothetical experiment and were studied the results obtained in ideal and real condition. The

simulation was made with an initial pressure in the dosing cell equal to 4 MPa and a temperature of 298.15 K, the results refer to the Peng-Robinson equation of state.

Firstly, was compared the variation of the compressibility factor at high pressure and low temperature respect the one in ideal condition (low pressure and high temperature). From the Fig. 29 it is possible to see that the behaviour of Z described before is verified. Indeed, when ideal conditions are imposed the value of Z is constant and equal to 1. While, in the other case it is possible to observe a variation of the parameter.

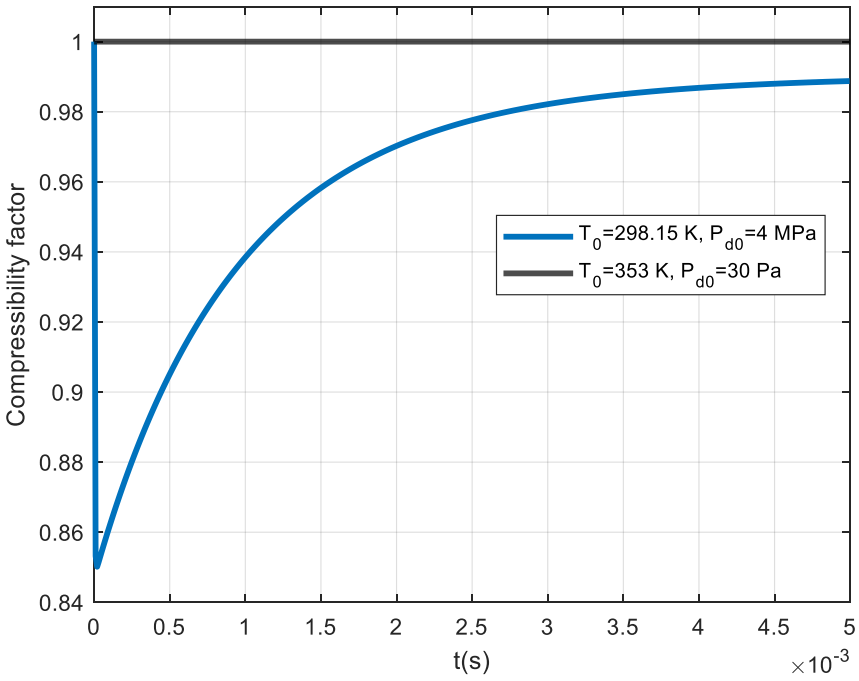

***Figure 29**: Compressibility factor (Z) behaviour*

One of the assumptions used to describe the behaviour of a real gas is that the inter-molecular forces are evenly distributed within the gas but close to a wall the molecules have higher attractive force on the gas side than on the wall side.

Since the gas pressure is caused by the molecules colliding with its surrounding walls, in general the pressure calculated with an equation of state is lower compared to the one obtained with the ideal gas law.

Furthermore, since the compressibility factor assume values which are lower than zero the concentration of the compound in the gas phase, considering the real behaviour, should be greater respect the one of the ideal case.

Studying the pressure and the concentration response in the Fig. 30, it is possible to say that the results obtained in the model correspond with the theoretical behaviour described before.

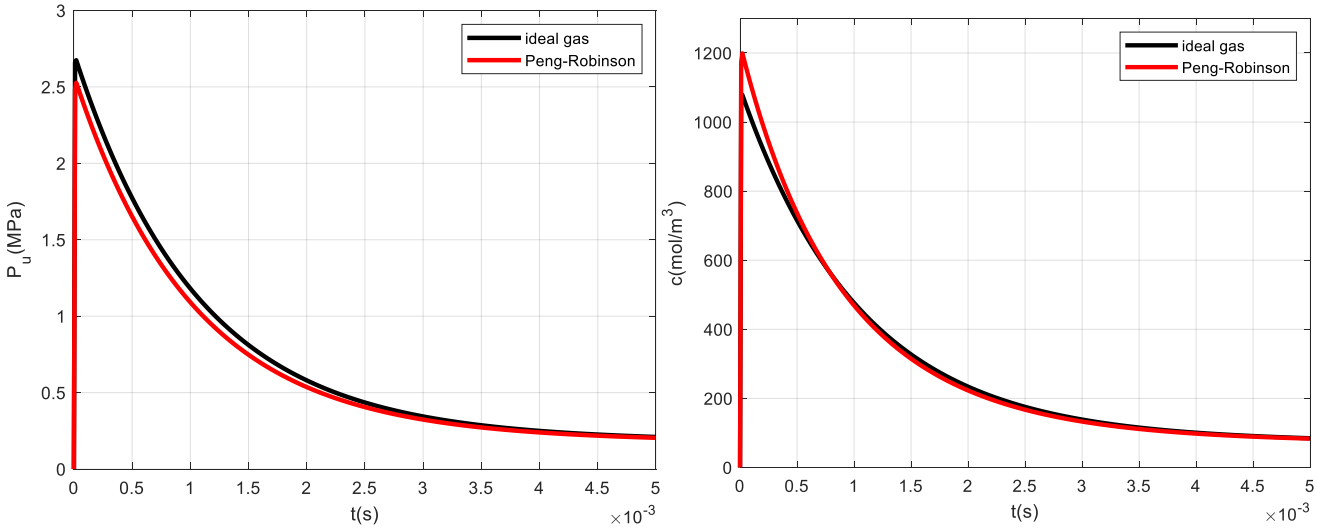

Figure 30: *Pressure and concentration response in the uptake cell considering the ideal gas law and the Peng-Robinson equation*

3.5.3 Case study: Comparison of adsorption curves in real and ideal conditions

The operative pressure for an adsorption process represents one of the main parameters which affects the adsorption capacity of a material.

In this section is studied the effects of the compressibility factor on the kinetic related to the adsorption of carbon dioxide. In particular, was calculated the variation of the reduced pressure in ideal gas condition and then was compared with the results obtained whit the two equations of state (Peng-Robinson and Van der Waals equations) implemented inside the model.

The simulation was done assuming isothermal condition with an initial pressure in the dosing cell of 8.5 bar. Then, was assumed a non-linear equilibrium and was used the Langmuir parameters reported by Park et al. (2016) related to the adsorption of CO_2 on 13X zeolite.

***Table 8**: Parameters used in the simulation (Park, Ju, Park, & Lee, 2016)*

Volume of solid	V_s	1.71E-08	m^3
Initial temperature	T_0	293	K
Diffusivity	D	8.45E-12	m^2/s
Radius	R	1.6	mm
Pressure in dosing cell	$P_{d,0}$	850.5	kPa
Pressure in uptake cell	$P_{u,0}$	817.1	kPa
q_s		8545.6	mol/m^3
b		1.37E-01	kPa^{-1}

Analysing the Fig. 31 is possible to observe how both equations of state cause a deviation in the trend of the reduced pressure. This means that the gas compressibility factors have a significant effect on high-pressure adsorption. The Peng-Robinson equation is the one which gives the biggest difference respect the ideal condition, indeed, in this case, there is an average deviation of the results of the 36%.

While, for the van der Waals equation, the deviation respects the ideal condition stands at 30%. Anyway, what is evident is the fact that the use of the ideal gas law for high pressure adsorption analysis, despite its simplicity, can leads to an erroneous interpretation of the results.

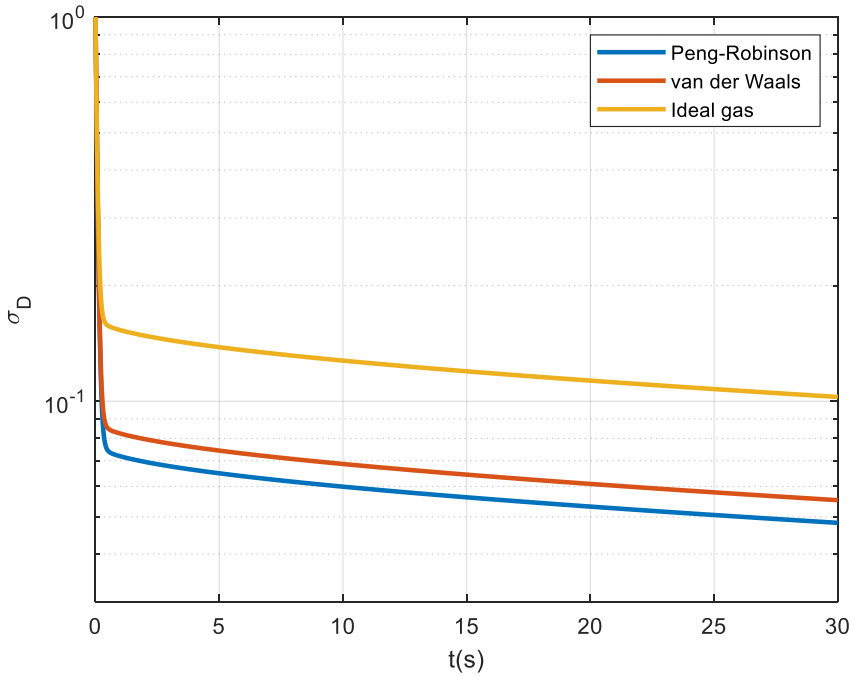

***Figure 31**: uptake curves for the three cases*

4. Modeling of a Volumetric system in a double-branch apparatus

In general, the majority of engineering applications related to an adsorption process occurs above room temperature and at high pressures. Reliable and accurate adsorption measurements under these conditions, as was already states, are critical to the design and characterization of new materials for adsorption. This is especially the case when gases with very low uptakes are studied.

Adsorption measurement at room temperature and high pressure always come with an inherent uncertainty in the collected data. The uncertainty is mostly due to the imprecision of the measurement device as well as to insufficient control of other parameters like temperature fluctuations.

In a volumetric apparatus different parameter can affect the pressure of the system, such as volume and temperature, and this led to a variation of the final results, as well. The accuracy of volumetric adsorption measurements is proportional to the accuracy of the pressure transducers used for the analysis. Indeed, even the best pressure transducers are limited in their ability to provide both wide range and high-resolution measurements at the same time. To overcome this shortcoming, differential pressure adsorption can be used. A differential error analysis on the collected data is useful in such cases because it can provide better insight into the reliability of the data.

In a classic volumetric apparatus (*Sieverts apparatus*) one absolute pressure transducer is used to measure and record pressure changes in the uptake volume before and after gas expansion and until the adsorption process reaches the equilibrium. This imposes a significant constraint on high pressure adsorption because it requires high accuracy over a long range of pressures.

Indeed, when the adsorbate has low affinity for the adsorbent, then a large amount of adsorbent is required to eliminate the errors in the pressure change measurements.

This problem is overcome in the differential pressure adsorption design. This apparatus incorporates two identical cells, connected to the sides of a differential pressure transducers, which have much higher accuracy (ca. 25 times) than direct pressure transducers.

The adsorbent is placed in the sample cell while the other, empty vessel acts as a reference. Dosing both the legs simultaneously with the adsorbate and measuring the differential pressure, obviates the need to make an accurate absolute pressure measurement (Qajar, Peer , Rajagopalan, & Foley, 2012).Each experiment is performed first through the charging of the

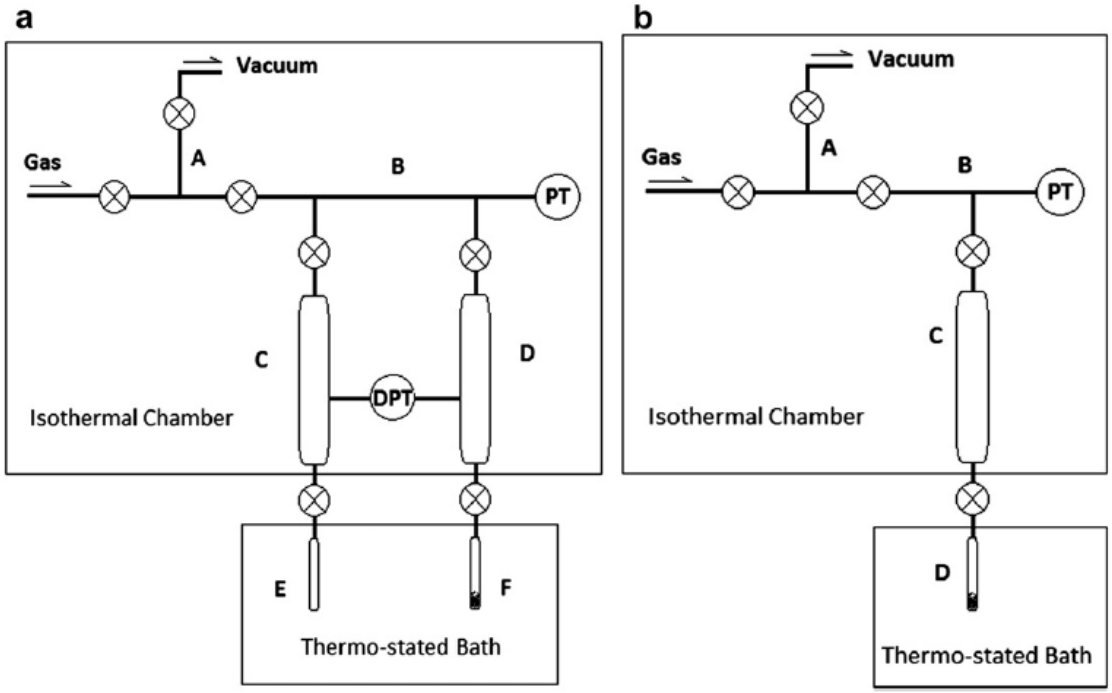

***Figure 32**: (a) Schematic representation of a high differential pressure apparatus, (b) Schematic representation of a Sieverts apparatus (Qajar, Peer , Rajagopalan, & Foley, 2012)*

two dosing cells with the gas to be studied. The instantaneous gas pressure in the two cells is measured by an absolute pressure transducer.

After reaching thermal equilibrium, the gas in the two manifolds was simultaneously expanded into the uptake cells. The difference between the pressures of the sample cell and the reference cell represented the gas uptake by the adsorbent.

4.1 Process Description & Mathematical Model

The mathematical model for a double-branch apparatus is made through the implementation of the different equations for the two sections of the system, the one related to the sample cell and the one related to the reference cell. Some assumptions were made in order to simplify the model:

- Temperatures of sample and reference uptake cells are equal $T_u = T_{u,s} = T_{u,r}$
- Temperatures of sample and reference dosing cells are equal $T_d = T_{d,s} = T_{d,r}$
- Volumes of sample and reference uptake cells are equal $V_u = V_{u,s} = V_{u,r}$
- Volumes of sample and reference dosing cells are equal $V_d = V_{d,s} = V_{d,r}$

For the sample section the equation used are the same saw in the Chapter 3 related to a single-branch apparatus.

Instead, for the reference section the mathematical model was made considering as unique physical phenomenon the expansion of the gas from the dosing cell in the uptake cell, without any adsorption of gas inside a material:

$$\frac{dn_r}{dt} = \chi_t \chi (P_{d,r}^2 - P_{u,r}^2) \tag{4.1}$$

Where $P_{d,r}$ and $P_{u,r}$ are the pressures in the dosing and uptake cells related to the reference section. The mass balance in the uptake and reference cells are the following:

$$\varepsilon V_u \frac{dc_r}{dt} = \frac{dn_r}{dt} \tag{4.2}$$

$$\frac{dn_r}{dt} = -\frac{V_d}{R_g T_d} \frac{dP_{d,r}}{dt} \tag{4.3}$$

Then, it is possible to calculate the difference in pressure between the sample and reference sides:

$$dP = P_{d,r} - P_{d,s} \tag{4.4}$$

For a double-branch apparatus, the experiments can be done in two ways:

- Differential mode: the valves on both sides are opened simultaneously and the differential pressure is read
- Absolute mode: the system works as a conventional single-branch apparatus; the pressure in the reference side is maintained constant and is open only the valve of the sample side, then the pressure variation in the sample side is calculated as the sum of the pressure of the reference side plus dP

In the differential mode, since the variable measured is dP, the form of the reduced pressure now changes and became function of the differential pressure:

$$\sigma_D^d = \frac{dP - dP_\infty}{dP_0 - dP_\infty} \tag{4.5}$$

Also in this case, the parameter varies between 1 and 0, it has a slope that is equal to the reduced pressure express with the absolute pressure, but with a profile which is shifted up. The advantage of using differential mode is the fact that now from the trend of the reduced pressure it could be better identify, for example, the effect of heat on the kinetics, or to have a better estimation of the valve constant.

4.2 Analysis of results for a double-branch apparatus

The new model was tested in order to observe how the pressure varies between the sample side and the reference side. In particular, the analysis was made considering the adsorption of hydrogen in isothermal condition.

The choice of the hydrogen is due to the fact that this substance represents a renewable energy source for transport applications that can be used to replace fossil fuels.

The simulation was carried out considering a pressure in the dosing cell equal to 1.4 bar and vacuum condition in the uptake cell, while the temperature was set to 298.15 K. To take into account the behaviour of a weakly adsorbed gas was used a value of the intracrystalline diffusivity of $2 \times 10^{-14}\ \frac{m}{s^2}$.

Finally, was recorded the variation of the pressure in the dosing cells in the sample and in the reference side, and the trend of the dP.

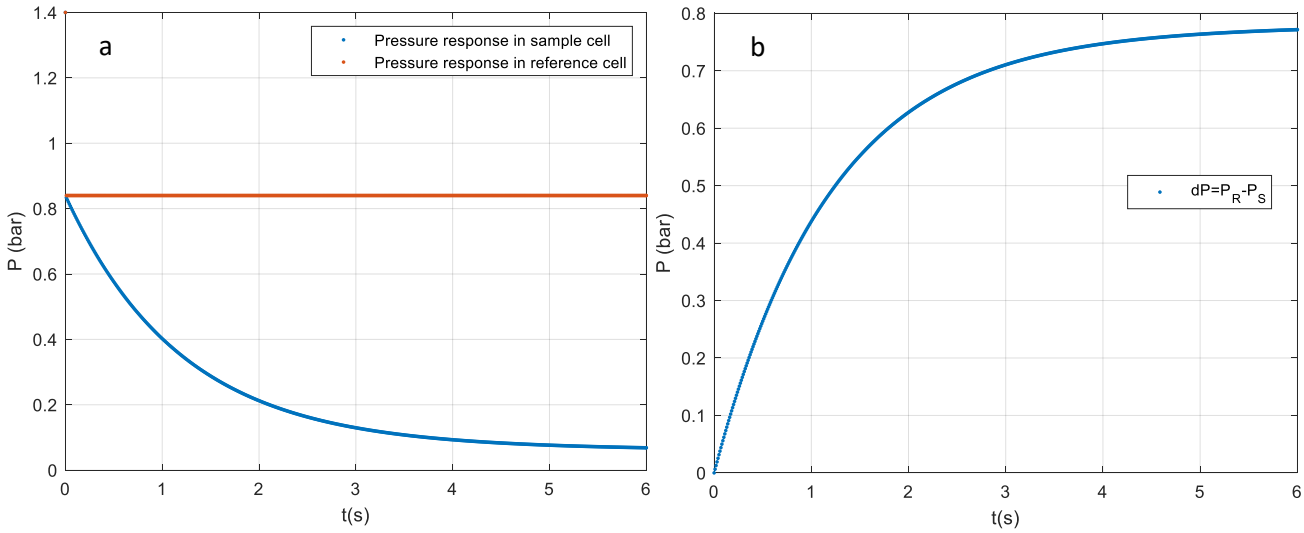

***Figure 33**: a) pressure response in the two sides; b) trend of dP*

Observing the red curve in the Fig. 33a, which refers to the pressure in the reference cell, it is possible to appreciate how the pressure of the system reaches practically instantaneously the equilibrium, this particular behaviour is present not only because was considered an instantaneous valve (an opening time equal to zero), but also because, as was already said, the only physical phenomenon present is the expansion of the gas.

While the blue curve, which refers to the sample, in the short time the trend is basically the same of the reference side, but when the gas reaches the material is possible to see a further pressure drop due to the adsorption of the gas.

A particular situation that could happen during adsorption experiments done with a differential apparatus, is when is present a little delay in the opening of the two valves in the reference and sample sides. In this sense, in order to simulate this phenomenon, the valve on the reference side was forced to open with a delay of 0.3 s.

As show in the Fig. 34, in this condition the trend of the differential pressure changes, because at the beginning of the experiment the pressure in the reference side remains constant, while the one in the sample side starting to decrease, this leads to the generation of a particular peak in the trend of dP.

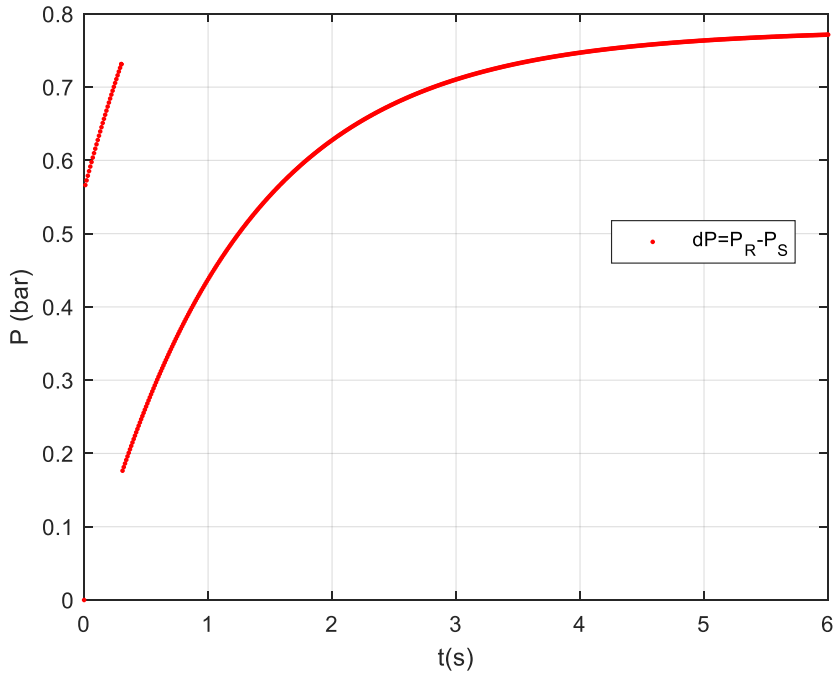

***Figure 34**: trend of dP with a delay of the valve of 0.3 s*

Some case studies seen for a single-branch apparatus are now analysed, focusing on what could be the possible advantages that a differential apparatus could have in the kinetic measurement.

As examples, were reported the cases study presented in the Section 3.2.3 and in the Section 3.4.3 related to the adsorption of CO_2 on 13X zeolite. The parameters used in the simulation are the same reported in the Table 5 and Table 7.

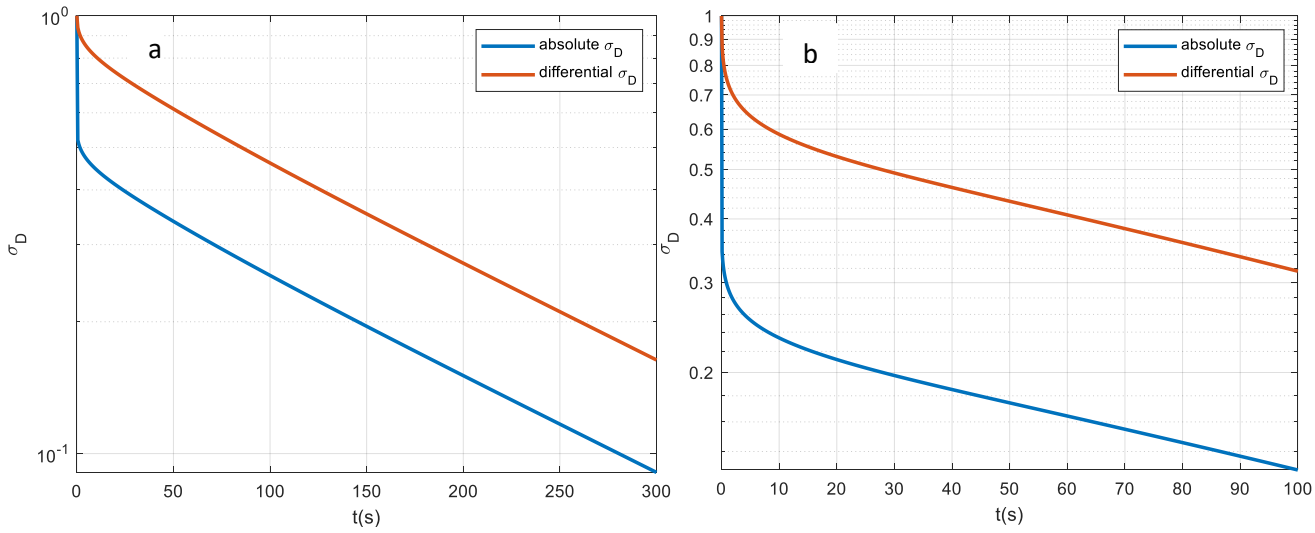

***Figure 35**: trends of uptake curves; a) Case study of Section 3.2.3; b) Case study of Section 3.4.3*

In the Fig. 35 are reported the trends of the reduced pressure, for the same process, calculated for the differential and absolute mode. The use of the differential reduced pressure seems gives no further information respect the absolute one in the long-time mass transfer region, in particular related to the effect of the heat. For the Fig. 35a this could be related to the high value of α, so that even with the differential technique the heat transfer effect is not highlighted.

Instead, analysing the short-time region, it is possible to observe how the differential mode highlight better the effect of the valve on the kinetic of the process, so it could be useful in order to have a better estimation of this parameter.

5. Conclusions and future work

In this work, was developed a mathematical model for the analysis of adsorption processes. The objective was the implementation of the different equations related to mass and energy balance in order to study the kinetic of the process in any operative conditions.

To assess the reliability of the model different comparative analysis were carried out. For example, in the Section 3.1.2, the comparison was made starting from the analytical solutions developed by Brandani (1998) for the piezometric method.

While, in the Section 3.2.2 and 3.4.2, where the effect of non-isothermality was discussed, the validation of the model was made through the adjustment of the parameters α and β in order to reach the isothermal condition. And was demonstrated that this occurs when $\alpha \to \infty$ (infinitely high heat transfer coefficient) or $\beta \to 0$ (infinitely large heat capacity).

The implementation of the Langmuir isotherm, used to describe a non-linear equilibrium, and the equations of state, particularly important when a high-pressure adsorption is made, represent a further improvement of the model.

Then, the model built for a single-branch apparatus was adapted in order to design a volumetric differential apparatus, which represents an innovative system for the measurement of adsorption equilibrium and kinetics.

In general, it is possible to affirm how the model is able to describe the physical-chemical phenomenon of the adsorption with accuracy.

The cases study analysed represent a further confirmation of the robustness of the model, as the results provided by the latter are in agreement with what was expected. Although a further comparison with laboratory data would also be essential.

gPROMS was found to be an efficient simulation tool for process model development. In comparison to other commercial modeling software packages, gPROMS offers a more flexible and versatile modeling environment with its user-friendly interface.

Although the model turns out to be reliable, it is necessary a further work in a number of areas. Firstly, it could be useful the creation of a simple interface that is able to guide the user in using the model, minimizing any type of error during the insertion of the parameters, also giving the possibility to insert the different conditions (e.g. non-isothermality, type of isotherm to use) based on the analysis the user wants to do.

Then, is needed the implementation of terms which take into account the effects of kinetic energy on adsorption dynamics. Indeed, inside the energy balances, which in this case are only enthalpic balances, must be included also the term related to the variation of the kinetic energy.

Another important aspect that needs to be improved is the one related to the type of equation of state used to describe the real behaviour of the gas. Indeed, even if the cubic equation of state, such as those included in the model, have the great advantage of being easily implementable, their unreliability in describing the behaviour of substances in particular conditions of pressure and temperature is known (Kunz, Klimeck, Wagner, & Jaeschke, 2007). In this sense, a possible solution could be the implementation of the equation of state developed by Span & Wagner (1996). The equation gives very accurate results, even in the region around the critical point. For instance, it is used in the *NIST Chemistry WebBook.*

Appendix A

gPROMS code for a single-branch volumetric apparatus

```
PARAMETER
Vs          AS REAL     #m^3              Volume of sample
eps         AS REAL     #                 Void fraction
Vu          AS REAL     #m^3              Volume of uptake cell
Vd          AS REAL     #m^3              Volume of dosing cell
Du          AS REAL     #m^3              Diameter of uptake cell
t_w         AS REAL     #m                thickness of cell
R_gas       AS REAL DEFAULT 8.3145
T0          AS REAL     #K                Initial Temperature
T_inf       AS REAL     #K                Bulk temperature
T_ref       AS REAL     #K                Reference temperature
D0          AS REAL     #m^2/s            Diffusivity coefficient
Rp          AS REAL     #m                Radius of crystals
K0          AS REAL
q_0         AS REAL     #mol/m^3          initial adsorbed conc.
c_0         AS REAL     #mol/m^3          initial gas conc.
chi         AS REAL     #mol/Pa/s         Valve constant
chi_t       AS REAL     #                 opening valve function
q_inf       AS REAL     #mol/m^3          final adsorbed conc.
Pu_0        AS REAL     #Pa               Initial pressure uptake
P_inf       AS REAL     #Pa               Equilibrium pressure
Pd_0        AS REAL     #Pa               Initial pressure dosing
```

```
cp_s      AS REAL    #J/(kg K)        heat capacity sample
E1        AS REAL    #J/mol           Heat of adsorption
E2        AS REAL    #J/mol           Heat of adsorption
rho_s     AS REAL    #kg/m^3          density of sample
h_s       AS REAL    #W/(m^2 K)       heat transfer sample
a_s       AS REAL    #1/m             Particle A/V
h_w       AS REAL    #W/(m^2 K)       heat transfer gas->wall
a_w1      AS REAL    #1/m             ratio int surface to vol
C1        AS REAL    #                Coeff. heat cap. PERRY
C2        AS REAL    #                Coeff. heat cap. PERRY
C3        AS REAL    #                Coeff. heat cap. PERRY
C4        AS REAL    #                Coeff. heat cap. PERRY
C5        AS REAL    #                Coeff. heat cap. PERRY
U         AS REAL    #W/(m^2 K)       overall heat transfer
a_a       AS REAL    #1/m             ratio of log surf to vol
a_w2      AS REAL    #1/m
cp_w      AS REAL    #J/(kg K)        heat capacity of wall
rho_w     AS REAL    #kg/m^3          density of wall
wg        AS REAL    #                Compressibility factor
Tc        AS REAL    #                Critical Temperature
Pc        AS REAL    #                Critical Pressure
m         AS REAL
a_vdW     AS REAL    #                cohesion pressure
b_vdW     AS REAL    #                co-volume
b_pr      AS REAL
b1_0      AS REAL    #                Langmuir parameter 1
```

```
b2_0        AS REAL     #                Langmuir parameter 2
q_s1        AS REAL     #                conc. of saturation 1
q_s2        AS REAL     #                conc. of saturation 2
Linear      AS REAL
Eos         AS REAL
Diff        AS REAL
MW          AS REAL     #                Molecular weight of gas
DISTRIBUTION DOMAIN
Radial      AS [0:Rp]
VARIABLE
q           AS DISTRIBUTION(Radial) OF Concentration
Pd          AS Pressure
Pu          AS Pressure
c_u         AS Concentration
c_d         AS Concentration
q_ave       AS Concentration
n           AS Moles
sig_d       AS no_type
T_s         AS Temperature
Td          AS Temperature
Tu          AS Temperature
Tw_u        AS Temperature
Tw_d        AS Temperature
H           AS Heat_of_adsorption
cp_g        AS heat_capacity
```

```
K          AS no_type
Z_u        AS Compressibility_factor
Z_d        AS Compressibility_factor
T_ru       AS no_type
T_rd       AS no_type
alfa_u     AS no_type
alfa_d     AS no_type
a_pr_u     AS no_type
a_pr_d     AS no_type
AA_u       AS no_type
AA_d       AS no_type
BB_u       AS no_type
BB_d       AS no_type
D          AS DISTRIBUTION (Radial) OF Diffusivity
D_ave      AS Diffusivity
b1         AS Langmuir_parameter
b2         AS Langmuir_parameter
mu         AS JT_coefficient
rho_gu     AS Density
rho_gd     AS Density

BOUNDARY
PARTIAL(q(0),Radial) = 0;
IF Linear =0 THEN
q(Rp)-q_0 =K * (c-c_0);
ELSE
```

```
q(Rp)=(q_s1*b1*Pu)/(1+b1*Pu);

#((q_s1*b1*Pu)/(1+b1*Pu))+((q_s2*b2*Pu)/(1+b2*Pu));

END

EQUATION

#-------------------GOVERNING EQUATIONS-----------------------

Vs * $q_ave + ((eps*Vu)/(R_gas*Tu)) * $Pu =-(Vd/(R_gas*Td)) *
$Pd;

$n = -((Vd/(R_gas*Td)) * $Pd);

IF Pd_0<500 THEN

$n =chi* chi_t *(Pd_0+Pu_0)* (Pd - Pu); # FOR SMALL P. DIFF.

ELSE

$n =chi* chi_t *(Pd^2-Pu^2);

END

FOR rad:=0|+ to Rp|- DO

$q(rad) = (1/rad^2) *
(PARTIAL((D(rad)*rad^2*PARTIAL(q(rad),Radial)),Radial));

END

$q_ave =((3/Rp) * PARTIAL(D(Rp)*q(Rp),Radial));

c_u=Pu/(R_gas*Tu*Z_u);

c_d=Pd/(R_gas*Td*Z_d);

sig_d=(Pd-P_inf)/(Pd_0-P_inf);
#-----------------------------------------------------------

#--------------------ENERGY BALANCES-------------------------

K=K0*EXP((-E/(R_gas)*(1/T_s-1/T_ref)));

b1=b1_0*EXP((-E1/(R_gas)*(1/T_s)));

b2=b2_0*EXP((-E2/(R_gas)*(1/T_s)));

IF h_s>1000 THEN
```

```
$T_s=$Td=$Tu=$Tw_d=$Tw_u=0;

ELSE

$T_s = ((h_s * a_s) / (rho_s * cp_s)) * (Tu - T_s) + (-H/(cp_s
* rho_s)) * $q_ave;

$Td * rho_gd= ((h_w * a_w1) / (cp_g)) * (Tw_d - Td);

$Tu * rho_gu = ((h_s * a_s * (1-eps))/(eps * cp_g)) * (T_s -
Tu) + ((h_w * a_w1) / (eps * cp_g )) * (Tw_u - Tu);

$Tw_u =((h_w * a_w2)/(rho_w * cp_w))*(Tu - Tw_u)+((U *
a_a)/(rho_w * cp_w)) * (T_inf - Tw_u);

$Tw_d=((h_w * a_w2)/(rho_w * cp_w))*(Td - Tw_d)+((U *
a_a)/(rho_w * cp_w)) * (T_inf - Tw_d);

END

cp_g=(C1+C2*(((C3/Tu)/(SINH(C3/Tu)))^2)+C4*(((C5/Tu)/(SINH(C5/
Tu)))^2))/(MW*1000);

H=(((q_s1*b1*E1)/(1+b1*Pu)^2)+((q_s2*b2*E2)/(1+b2*Pu)^2))/((((
q_s1*b1)/(1+b1*Pu)^2)+((q_s2*b2)/(1+b2*Pu)^2)));

#-------------------------------------------------------------

#--------------------EQUATIONS OF STATE-----------------------

IF Eos=1 THEN

Z_u^3-
(1+((b_vdW*Pu)/(R_gas*Tu)))*Z_u^2+((a_vdW*Pu)/(R_gas*Tu)^2)*Z_
u-(((a_vdW*Pu)/(R_gas*Tu)^2)*((b_vdW*Pu)/(R_gas*Tu)))=0;

Z_d^3-
(1+((b_vdW*Pu)/(R_gas*Tu)))*Z_d^2+((a_vdW*Pu)/(R_gas*Tu)^2)*Z_
d-(((a_vdW*Pu)/(R_gas*Tu)^2)*((b_vdW*Pu)/(R_gas*Tu)))=0;


ELSE

Z_u^3-(1-BB_u)*Z_u^2+(AA_u-3*BB_u^2-2*BB_u)*Z_u-(AA_u*BB_u-
BB_u^2-BB_u^3)=0;


Z_d^3-(1-BB_d)*Z_d^2+(AA_d -3*BB_d^2-2*BB_d)*Z_d-(AA_d*BB_d-
BB_d^2-BB_d^3)=0;
```

```
END

AA_u =a_pr_u*Pu/((R_gas*Tu)^2);

BB_u =b_pr*Pu/(R_gas*Tu);

T_ru=Tu/Tc;

alfa_u=(1 + m*(1 - sqrt(T_ru)))^2;

a_pr_u=0.45724*(R_gas*Tc)^2/Pc*alfa_u;

AA_d =a_pr_d*Pd/((R_gas*Td)^2);

BB_d =b_pr*Pd/(R_gas*Td);

T_rd=Td/Tc;

alfa_d=(1 + m*(1 - sqrt(T_rd)))^2;

a_pr_d=0.45724*(R_gas*Tc)^2/Pc*alfa_d;

IF Eos=1 THEN

mu/1e6=(((2*a_vdw)/(R_gas*Tu))-b_vdw)/(cp_g*MW);

ELSE

(mu*c_u)/1e6=(Tu/(Z_u*cp_g*MW))*(((((-
2*a_pr_u*Pu)/(R_gas^2*Tu^3))*(BB_u-Z_u)+((-
b_pr*Pu)/(R_gas*Tu^2))*(6*BB_u*Z_u+2*Z_u-3*BB_u^2-2*BB_u+AA_u-
Z_u^2))/(3*Z_u^2+2*(BB_u-1)*Z_u+(AA_u-2*BB_u-3*BB_u^2))));

END

rho_gu=c_u*MW;

rho_gd=c_d*MW;
#-------------------------------------------------------------
IF Diff =0 THEN

D/D0=1;

ELSE

D/D0=1/(1-(q(Rp)/q_s1));

#(((1+b1*Pu)*(1+b2*Pu))*(q_s1*b1*(1+b2*Pu)+q_s2*b2*(1+b1*Pu)))
/((q_s1*b1*(1+b2*Pu)^2)+(q_s2*b2*(1+b1*Pu)^2));

END
```

```
D_ave=(3/Rp^3)* INTEGRAL (rad:=0:Rp;(D(rad)*rad^2));
```

Appendix B

gPROMS code for a double-branch volumetric apparatus

```
PARAMETER
Vs          AS REAL     #m^3
eps         AS REAL
Vu          AS REAL     #m^3
Vd          AS REAL     #m^3
Du          AS REAL     #m^3
t_w         AS REAL     #m
R_gas       AS REAL DEFAULT 8.3145
T0          AS REAL     #K
T_inf       AS REAL     #K
T_ref       AS REAL     #K
D0          AS REAL     #m^2/s
Rp          AS REAL     #m
K0          AS REAL
q_0         AS REAL     #mol/m^3
c_0         AS REAL     #mol/m^3
chi         AS REAL     #mol/Pa/s
chi_t       AS REAL
q_inf       AS REAL     #mol/m^3
Pu_0        AS REAL     #Pa
P_inf       AS REAL     #Pa
```

```
Pr_inf    AS REAL
Pd_0      AS REAL    #Pa
dP_0      AS REAL    #Pa
dP_inf    AS REAL    #Pa
cp_s      AS REAL     #J(kg K)
E1        AS REAL     #J/mol
E2        AS REAL     #J/mol
rho_s     AS REAL     #kg/m^3
h_s       AS REAL     #W/(m^2 K)
a_s       AS REAL     #1/m
h_w       AS REAL     #W/(m^2 K)
a_w1      AS REAL     #1/m
C1        AS REAL
C2        AS REAL
C3        AS REAL
C4        AS REAL
C5        AS REAL
cp_g      AS REAL     #J(kg K)
U         AS REAL     #W/(m^2 K)
a_a       AS REAL     #1/m
a_w2      AS REAL     #1/m
cp_w      AS REAL     #J(kg K)
rho_w     AS REAL     #kg/m^3
wg        AS REAL
Tc        AS REAL
Pc        AS REAL
```

```
m           AS REAL
a_vdW       AS REAL
b_vdW       AS REAL
b_pr        AS REAL
a_prr       AS REAL
Tu_r        AS REAL
T_rr        AS REAL
alfa_r      AS REAL
b1_0        AS REAL
b2_0        AS REAL
q_s1        AS REAL
q_s2        AS REAL
Equilbrium  AS REAL
Diff        AS REAL
Eos         AS REAL
MW          AS REAL
DISTRIBUTION DOMAIN
Radial   AS [0:Rp]
VARIABLE
q           AS DISTRIBUTION(Radial) OF Concentration
Pd          AS Pressure
Pd_r        AS Pressure
Pu          AS Pressure
Pu_r        AS Pressure
c_u         AS Concentration
```

```
c_d       AS Concentration
c_r       AS Concentration
q_ave     AS Concentration
n         AS Moles
n_r       AS Moles
sig_d     AS no_type
sig_dr    AS no_type
ssig_d    AS no_type
dP        AS Pressure
T_s       AS Temperature
Td        AS Temperature
Tu        AS Temperature
Tw_u      AS Temperature
Tw_d      AS Temperature
H         AS Heat_of_adsorption
cp_g      AS heat_capacity
K         AS no_type
Z_u       AS Compressibility_factor
Z_r       AS Compressibility_factor
T_ru      AS no_type
alfa_u    AS no_type
a_pr_u    AS no_type
AA_u      AS no_type
BB_u      AS no_type
AA_r      AS no_type
BB_r      AS no_type
```

```
D          AS DISTRIBUTION (Radial) OF Diffusivity
D_ave      AS Diffusivity
b1         AS Langmuir_parameter
b2         AS Langmuir_parameter
mu         AS JT_coefficient
rho_gu     AS Density
rho_gd     AS Density
BOUNDARY
PARTIAL(q(0),Radial) = 0;
IF Equilbrium =0 THEN
q(Rp)-q_0 =K * (c_u-c_0);
ELSE
q(Rp) =((q_s1*b1*Pu)/(1+b1*Pu))+((q_s2*b2*Pu)/(1+b2*Pu));
#(q_s1*b1*Pu)/(1+b1*Pu)
END
EQUATION
#----------------GOVERNING EQUATIONS SAMPLE SIDE--------------
Vs * $q_ave +  ((eps*Vu) * $c_u) =-(Vd/(R_gas*Td)) * $Pd;
$n = -((Vd/(R_gas*Td)) * $Pd);
IF Pd_0<500 THEN
$n =chi*chi_t*(Pd_0+Pu_0)* (Pd - Pu);  #FOR S. P. DIFF.
ELSE
 $n =chi*chi_t*(Pd^2-Pu^2);
END
FOR rad:=0|+ to Rp|- DO
```

```
$q(rad) = (1/rad^2) *
(PARTIAL((D(rad)*rad^2*PARTIAL(q(rad),Radial)),Radial));

END

$q_ave =((3/Rp) * PARTIAL(D(Rp)*q(Rp),Radial));

c_u=Pu/(R_gas*Tu*Z_u);

c_d=Pd/(R_gas*Td*Z_d);

sig_d=(Pd-P_inf)/(Pd_0-P_inf);
#-------------------------------------------------------------



#---------------------ENERGY BALANCES--------------------
K=K0*EXP((-E1/(R_gas)*(1/T_s-1/T_ref)));

b1=b1_0*EXP((-E1/(R_gas)*(1/T_s)));

b2=b2_0*EXP((-E2/(R_gas)*(1/T_s)));

IF h_s>1000 THEN

$T_s=$Td=$Tu=$Tw_d=$Tw_u=0;

ELSE

$T_s = ((h_s * a_s) / (rho_s * cp_s)) * (Tu - T_s) + (-H/(cp_s
* rho_s)) * $q_ave;

$Td*rho_gd = ((h_w * a_w1) / (cp_g )) * (Tw_d - Td);

$Tu*rho_gu = ((h_s * a_s * (1-eps))/(eps * cp_g )) * (T_s -
Tu) + ((h_w * a_w1) / (eps * cp_g)) * (Tw_u - Tu);

$Tw_u =((h_w * a_w2)/(rho_w * cp_w))*(Tu - Tw_u)+((U *
a_a)/(rho_w * cp_w)) * (T_inf - Tw_u);

$Tw_d=((h_w * a_w2)/(rho_w * cp_w))*(Td - Tw_d)+((U *
a_a)/(rho_w * cp_w)) * (T_inf - Tw_d);

END

cp_g=(C1+C2*(((C3/Tu)/(SINH(C3/Tu)))^2)+C4*(((C5/Tu)/(SINH(C5/
Tu)))^2))/(MW*1000);

H=(((q_s1*b1*E1)/(1+b1*Pu)^2)+((q_s2*b2*E2)/(1+b2*Pu)^2))/((((
q_s1*b1)/(1+b1*Pu)^2)+((q_s2*b2)/(1+b2*Pu)^2)));
```

```
#-------------------------------------------------------------
#--------------------EQUATIONS OF STATE-----------------------

IF Eos=1 THEN

Z_u^3-
(1+((b_vdW*Pu)/(R_gas*Tu)))*Z_u^2+((a_vdW*Pu)/(R_gas*Tu)^2)*Z_
u-(((a_vdW*Pu)/(R_gas*Tu)^2)*((b_vdW*Pu)/(R_gas*Tu)))=0;

ELSE

Z_u^3-(1-BB_u)*Z_u^2+(AA_u-3*BB_u^2-2*BB_u)*Z_u-(AA_u*BB_u-
BB_u^2-BB_u^3)=0;

END

AA_u =a_pr_u*Pu/((R_gas*Tu)^2);

BB_u =b_pr*Pu/(R_gas*Tu);

T_ru=Tu/Tc;

alfa_u=(1 + m*(1 - sqrt(T_ru)))^2;

a_pr_u=0.45724*(R_gas*Tc)^2/Pc*alfa_u;


IF Eos=1 THEN

mu/1e6=(((2*a_vdw)/(R_gas*Tu))-b_vdw)/(cp_g*MW);

ELSE

(mu*c_u)/1e6=(Tu/(Z_u*cp_g*MW))*(((((-
2*a_pr_u*Pu)/(R_gas^2*Tu^3))*(BB_u-Z_u)+((-
b_pr*Pu)/(R_gas*Tu^2))*(6*BB_u*Z_u+2*Z_u-3*BB_u^2-2*BB_u+AA_u-
Z_u^2))/(3*Z_u^2+2*(BB_u-1)*Z_u+(AA_u-2*BB_u-3*BB_u^2))));

END

rho_gu=c_u*MW;

rho_gd=c_d*MW;
#-------------------------------------------------------------

IF Diff =0 THEN

D/D0=1;

ELSE
```

```
D/D0=(((1+b1*Pu)*(1+b2*Pu))*(q_s1*b1*(1+b2*Pu)+q_s2*b2*(1+b1*P
u)))/((q_s1*b1*(1+b2*Pu)^2)+(q_s2*b2*(1+b1*Pu)^2));
#1/(1-(q(Rp)/q_s1));

END

D_ave=(3/Rp^3)* INTEGRAL (rad:=0:Rp;(D(rad)*rad^2));


#---------------GOVERNING EQUATIONS REFERENCE SIDE------------

(eps*Vu)*$c_r =-(Vd/(R_gas*Td)) * $Pd_r;

$n_r = -((Vd/(R_gas*Td)) * $Pd_r);

IF Pd_0<500 THEN
$n_r =chi*chi_t*(Pd_0+Pu_0)* (Pd_r - Pu_r);

ELSE

 $n_r =chi*chi_t*(Pd_r^2-Pu_r^2);

END

c_r=Pu_r/(R_gas*Tu_r*Z_r);

sig_dr=(Pd_r-Pr_inf)/(Pd_0-Pr_inf);

IF Eos=1 THEN

Z_r^3-
(1+((b_vdW*Pu_r)/(R_gas*Tu_r)))*Z_r^2+((a_vdW*Pu_r)/(R_gas*Tu_
r)^2)*Z_r-
(((a_vdW*Pu)/(R_gas*Tu_r)^2)*((b_vdW*Pu)/(R_gas*Tu_r)))=0;

ELSE

Z_r^3-(1-BB_r)*Z_r^2+(AA_r-3*BB_r^2-2*BB_r)*Z_r-(AA_r*BB_r-
BB_r^2-BB_r^3)=0;

END

AA_r =a_prr*Pu_r/((R_gas*Tu_r)^2);

BB_r =b_pr*Pu_r/(R_gas*Tu_r);


dP=Pd_r-Pd;


ssig_d=(dP-dP_inf)/(dP_0-dP_inf);
```

References

Blackman, J., Patrick, J., & Colin, S. (2005). An accurate volumetric differential pressure method for the determination of hydrogen storage capacity at high pressures in carbon materials.

Brandani, S. (1998). Analysis of the Piezometric Method for the Study of Diffusion in Microporous Solids: Isothermal Case.

Brandani, S., & Hu, X. e. (2011). Flowrate correction for the determination of isotherms and Darken thermodynamics factors from Zero Length Column (ZLC) experiments.

Brandani, S., Brandani, F., Mangano, E., & Pullumbi, P. (2019). Using a volumetric apparatus to identify and measure the mass transfer resistance in commercial adsorbents.

Garg, D., & Ruthven, D. (1971). The effect of the concentration dependence of diffusivity on zeolitic sorption curves.

Gosling, I. (2005). Process simulation and modeling for industrial bioprocessing: Tools and techniques.

Kaario, O., Nuutinen, M., Lehto, K., & Larmi, M. (2010). Real Gas Effects in High-Pressure Engine Environment.

Karger, J., & Ruthven , D. (1992). Diffusion in Zeolites and Other Microporous Solids.

Kocirik, M. (1983). Analytical Solution of Simultaneous Mass and Heat Transfer in Zeolite Crystals under Constant-volume/Variable-pressure Conditions.

Kye, S., Jae, H., & Won, K. (1994). Fixed-Bed Adsorption for bulk component system. Non-equilibrium, non-isothermal and non-adiabatic model.

Mansour, E. M. (2020). Equation of state.

Martinez-Vertel, J. J., Villaquiràn-Vargas, A. P., Villar-Garcia, A., Moreno-Diaz, D. F., Rodriguez-Castelblanco, A. X., & Rodriguez, J. (2018). Polymer adsorption isotherms with NaCl and CaCl2 on kaolinite substrates.

MIC. (2005). Retrieved from https://www.micromeritics.com/Repository/Files/Gas_Adsorption_Apparatus_Poster.pdf

Montastruc, L., Floquet, P., Mayer, V., Nikov, I., & Domenech, S. (2010). Kinetic Modelig of Isothermal or Non-isothermal Adsorption in a Pellet: Application to Adsorption heat Pumps.

Nakhli, A., Bergaoui, M., Khalfaoui, M., Mollmer, J., Moller, A., & Lamine, A. B. (2014). Modeling of high pressure adsorption isotherm using statistical physics approach: lateral interaction of gases adsorption onto metal-organic framework HKUST-1.

Policicchio, A., Maccallini, E., Kalantzopoulos, G., Cataldi, U., Abate, S., Desiderio, G., & Agostino, R. (2013). Volumetric apparatus for hydrogen adsorption and diffusion measurements: Sources of systematic error and impact of their experimental resolutions.

PSe. (2004). *gPROMS introductory User Guide.*

PSe. (2005). Retrieved from https://www.psenterprise.com/

Ruthven, D. (1984). *Principles of Adsorption and Adosprtion Processes.*

Ruthven, D., & Garg, D. (1971). The effect of the concentration depedence of diffusivity on zeolitic sorption curves.

Ruthven, D., Lee, L.-K., & Yucel, H. (1980). Kinetics of Non-Isothermal Sorption in Molecular Sieve Crystals.

Sircar, S., Wang, C.-Y., & Lueking, A. (2013). Design of high pressure differential volumetric adsorption measurments with increased accuracy.

Stadie, N. (2013). *Appendix A: Experimental Adsorption Measurments.*

Tang, X., & Ripepi, N. (2016). Temperature-dependent Langmuir model in the coal and methane sorption process: Statistical relationship .

Tang, X., Ripepi, N., Stadie, N., Yu, L., & Hall, M. (2016). A dual-site Langmuir equation for accurate estimation of high pressure deep shale gas resources.

Wang, J.-Y., Mangano, E., Brandani, S., & Ruthven, D. (2020). A review of common practices in gravimetric and volumetric adsorption kinetic experiments.

Zielinski, J., Coe, C., Nickel, R., Romeo, A., Cooper, A., & Pez, G. (2007). High pressure sorption isotherms via differential pressure measurments.